Geology and U-Pb zircon geochronology and Pb isotope geochemistry of mid-Cretaceous plutonic rocks in the Mount Nansen map area (NTS 115I/3 and part of 115I/2)

Patrick J. Sack
Yukon Geological Survey

James L. Crowley
Boise State University

Venessa Bennett
Geomantia Consulting

Janet Gabites
University of British Columbia

Sack, P.J., Crowley, J.L., Bennett, V. and Gabites, J., 2022. Geology and U-Pb zircon geochronology and Pb isotope geochemistry of mid-Cretaceous plutonic rocks in the Mount Nansen map area (NTS 115I/3 and part of 115I/2). *In:* Yukon Exploration and Geology 2021, K.E. MacFarlane (ed.), Yukon Geological Survey, p. 185–215.

Abstract

The geology in the Mount Nansen area, of the Dawson Range, comprises a metamorphic basement overlain and intruded by mid and Late Cretaceous magmatic rocks. Mid-Cretaceous epithermal deposits are recognized in the Brown-McDade cluster in the south, and Late Cretaceous porphyry and epithermal occurrences in the centrally located Klaza cluster. Here we report eight new U-Pb zircon crystallization ages, two CA-TIMS and six LA-ICPMS, and Pb isotopic data for igneous feldspar from six samples. A 199.06 ± 0.96 Ma crystallization age demonstrates the host rock to the Brown-McDade deposit is the Late Triassic to Early Jurassic Minto suite. We report crystallization ages of 111 ± 1.8 Ma for the Dickson Hill porphyry, 107.96 ± 0.03 and 107.86 ± 0.03 Ma for the central and border phases of the Bow Creek granite, respectively, and 107.0 ± 0.72, 107.0 ± 0.78 and 107.5 ± 0.67 Ma for equigranular and porphyritic phases of the Dawson Range granodiorite. These ages confirm a mid-Cretaceous Whitehorse suite affinity for these rocks with porphyritic textures suggesting high-level emplacement. Feldspar Pb isotopic data of igneous rocks in the Mount Nansen area become more radiogenic with time and are distinct for Late Triassic to Early Jurassic plutonic rocks versus Cretaceous rocks. Cretaceous feldspar isotopic data broadly overlaps Pb isotopic values of galena from deposits throughout the Dawson Range suggesting coeval magmatic rocks are a significant source of metals.

* Patrick.Sack@yukon.ca

Regional geology

The Dawson Range area is broadly defined by the Yukon River to the east and north, the White River to the north and west and the Nisling River to the west and south (Fig. 1). The geology of the Dawson Range is predominantly composed of metamorphic Yukon-Tanana Paleozoic country rocks (Snowcap and Finlayson assemblages and the Simpson Range and Sulphur Creek metaplutonic suites) intruded by Late Triassic to Early Jurassic plutonic rocks (Pyroxene Mountain, Minto and Long Lake suites). These basement rocks were covered and intruded by Cretaceous volcanic and plutonic rocks (mid-Cretaceous Mount Nansen group and Whitehorse suite, and Late Cretaceous Carmacks group and Casino and Prospector Mountain suites; Ryan *et al.*, 2013, 2016, 2018; Sack *et al.*, 2021). The area is dissected by northwest and northeast trending faults with movement along the fault plane being Late Cretaceous and younger (e.g., Big Creek fault; Mottram *et al.*, 2020).

In the Dawson Range, Yukon-Tanana rocks were metamorphosed to greenschist and amphibolite facies as Late Triassic to Early Jurassic plutons were emplaced at >20 km depths during regional exhumation (Staples *et al.*, 2014; Clark, 2017; Gaidies *et al.*, 2020; Sack *et al.*, 2020). In contrast, mid-Cretaceous and younger rocks were emplaced at shallow crustal levels, and both plutonic and volcanic rocks of the mid-Cretaceous,

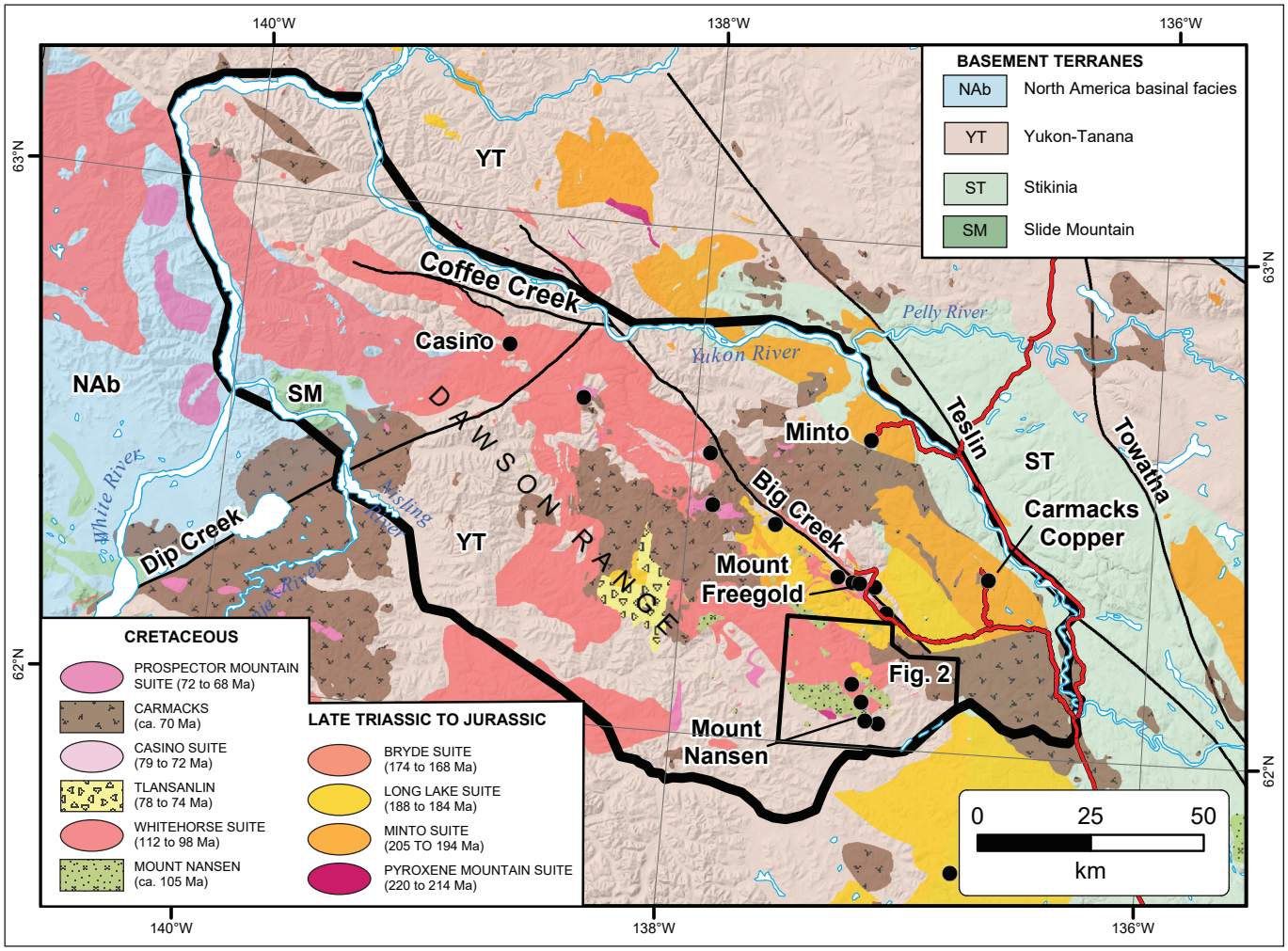

Figure 1. *Simplified regional geology map of the central Dawson Range (outlined in heavy black line). For this figure and Fig. 2, legend shape for layered units is a rectangle and for plutonic units is an oval. Significant mineral occurrences are shown with black circles. Regionally significant faults and mineral districts are labelled. Geology from YGS (2020).*

Late Cretaceous and Paleogene are preserved. From the perspective of mineral deposits, this means that the appropriate crustal level for development of porphyry systems (porphyry, epithermal and skarn deposits) is likely preserved throughout the Dawson Range for Cretaceous, but not Late Triassic to Early Jurassic, systems. The Mount Nansen area discussed in this paper is an example in the Dawson Range with both mid and Late Cretaceous porphyry system potential (e.g., Sawyer and Dickinson, 1976; Mortensen *et al.*, 2016; Mortensen and Friend, 2020; Lee, 2021).

Local geology

Basement

Basement rocks in the Mount Nansen area are primarily in the south and east (Fig. 2) where they are broadly folded along northeast trending fold axes (Sack *et al.*, 2021). With the local exception of the Snowcap amphibolite and the Minto suite, the basement has relatively low magnetic susceptibility (Table 1; Sack *et al.*, 2021) and shows up as magnetic lows on regional aeromagnetic maps (Aurora Geosciences and Bruce, 2020).

Yukon-Tanana terrane

Snowcap assemblage (PDS1 and PDS3)

The Snowcap assemblage is a Proterozoic to Devonian metasedimentary unit of quartzite and schist, and minor amphibolite of volcanic origin (Piercey and Colpron, 2009). In the Mount Nansen area, both the quartzite and schist are grey to white on weathered and fresh surfaces (Fig. 3a). The schist tends to be darker as the biotite content increases. The quartzite and schist have quartz, feldspar, muscovite, biotite and locally garnet. These rocks are strongly foliated and layered, and locally form a quartzofeldspathic schist difficult to distinguish from Simpson Range metagranitoid (MgSR). The magnetic susceptibility of the Snowcap quartzite and schist ranges from 18.10 to 0.01×10^3 SI units with a median value of 0.32 (Table 1). Snowcap amphibolite is layered dark green and white on weathered and fresh surfaces (Fig. 3b) and is fine to medium grained, equigranular and well foliated. The magnetic susceptibility of the Snowcap amphibolite ranges from 24.0 to 0.11×10^3 SI units with a median value of 4.09 (Table 1).

Finlayson assemblage (DMF1 and DMF2)

The Finlayson assemblage consists of mafic (DMF1) and felsic (DMF2) map units. The mafic unit is difficult to differentiate from the Snowcap amphibolite at the outcrop scale as the Finlayson amphibolite is also dark green, strongly foliated and locally compositionally layered. It is generally schistose, locally gneissic and more chloritic than the Snowcap amphibolite (PDS3). The magnetic susceptibility of the Finlayson amphibolite ranges from 2.93 to 0.04×10^3 SI units with a median value of 0.21 (Table 1) suggesting it may be a less magnetic unit than the Snowcap amphibolite. The felsic Finlayson unit is only found in 50 000 map scale units in the southwestern corner of the Mount Nansen map area (Fig. 2) where Ryan *et al.* (2016) describe it as a schistose, fine-grained felsic metavolcanic rock commonly with a fragmental texture. The felsic unit was deposited ca. 351 to 344 Ma (Joyce *et al.*, 2020).

Simpson Range metaplutonic suite (MgSR)

The Simpson Range metaplutonic suite is a biotite ± hornblende metagranodiorite. It is light grey to orange weathered and light grey fresh with local feldspar augen. It is well foliated and is locally compositionally banded with more mafic (biotite-hornblende-rich) and more felsic (quartz-feldspar-rich) layers making it difficult to distinguish from the quartzofeldspathic schist of the Snowcap assemblage. The Simpson Range metaplutonic suite (365 to 350 Ma) intruded Snowcap rocks and is slightly older to coeval with the Finlayson assemblage (Joyce *et al.*, 2020). The magnetic susceptibility of the Simpson Range metaplutonic suite ranges from 10.9 to 0.0005×10^3 SI units with a median value of 0.31 (Table 1).

Sulphur Creek metaplutonic suite (PgS)

One body of Sulphur Creek orthogneiss is mapped to the east of Victoria Creek (Fig. 2; Ryan et *al.*, 2016; Sack et *al.*, 2021) where it is a fine-grained, grey to pink alkali feldspar porphyritic monzonite that is moderately foliated (Fig. 3c). The magnetic susceptibility of this body ranges from 0.53 to 0.01 × 10³ SI units with a median value of 0.03 (Table 1).

Late Triassic to Early Jurassic plutons

Pyroxene Mountain suite (LTrPx)

The Pyroxene Mountain suite is medium-grained, foliated hornblende diorite to quartz diorite that intruded the Finlayson assemblage and locally the Snowcap assemblage (Ryan et *al.*, 2016). The magnetic susceptibility of the Pyroxene Mountain suite ranges from 0.41 to 0.12 × 10³ SI units with a median value of 0.26 (Table 1). The Pyroxene Mountain body on the south flank of Mount Nansen was intruded ca. 216 Ma (Colpron et *al.*, *in press*).

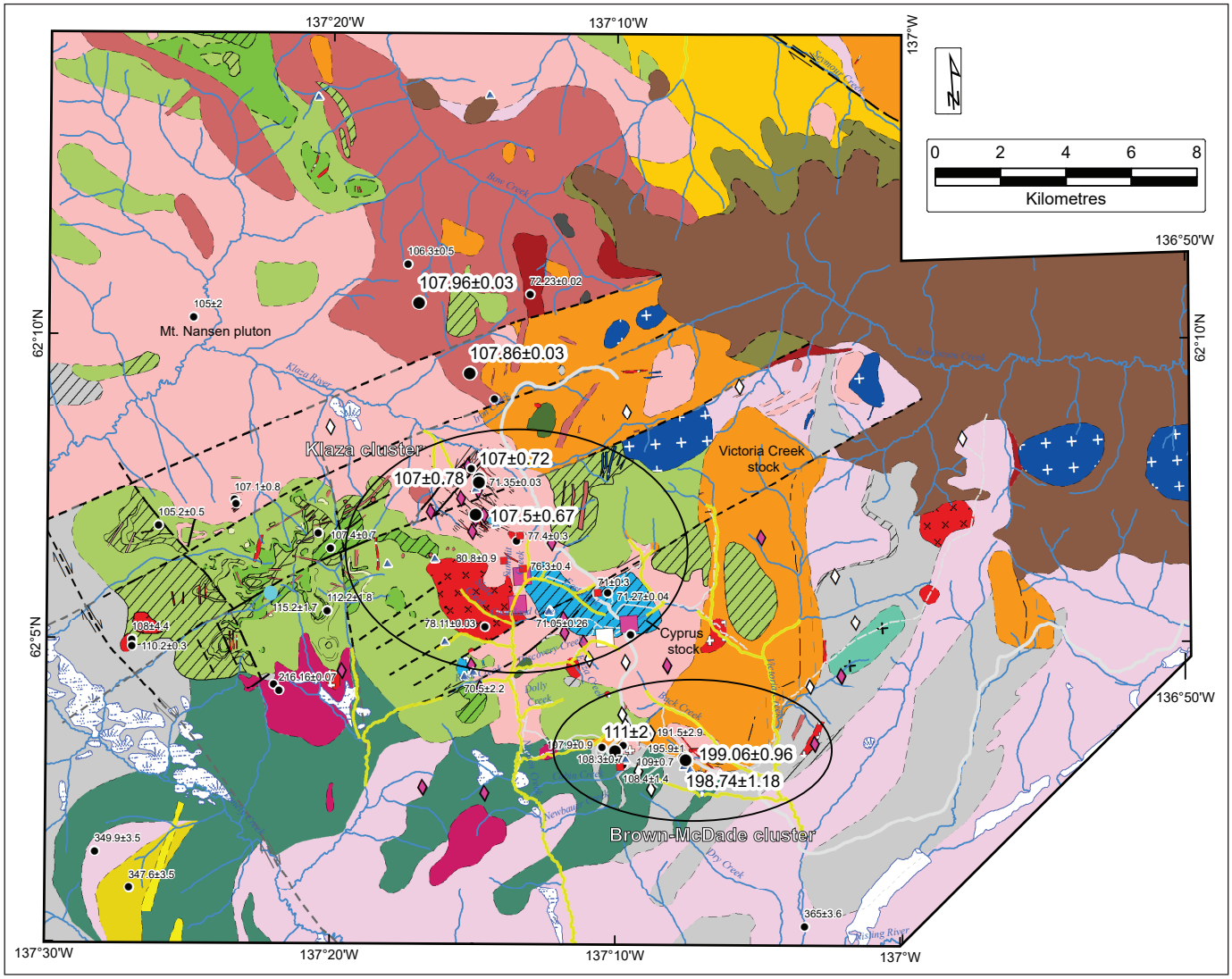

Figure 2. *Simplified geology of the Mount Nansen map area (NTS 115I/3 and part of 115I/2). Legend on following page. For Prospector Mountain suite and Mount Nansen group, units on map with angled hatching are breccia of dominantly same lithology as unhatched unit of same colour. U-Pb zircon ages presented in this paper are those shown with larger symbols and labelled with a larger font. Modified from Sack et al. (2021).*

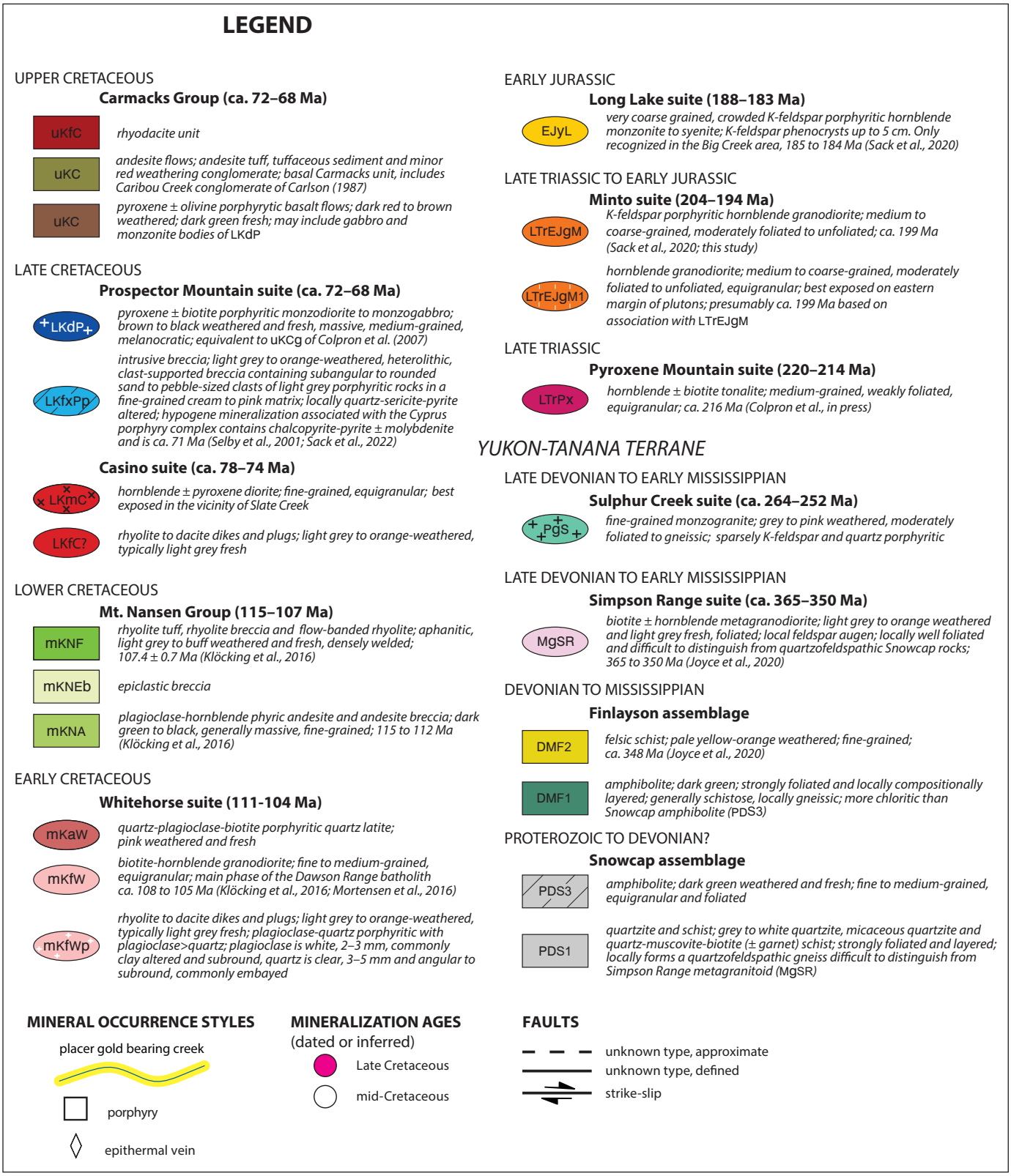

***Figure 2** continued.*

Table 1. *Magnetic susceptibility measurements from the Mount Nansen area mostly summarized by map unit. N = number of stations with a magnetic susceptibility measurement; each magnetic susceptibility measurement is the mean of five point measurements over a 1 to 2 m² area, within the same lithology. Data are in Appendix 1.*

	Map units	Mean	Median	Minimum	Maximum	Std dev	N	
Propsector Mountain (mafic)	LKdP	8.47	6.49	0.20	20.70	9.77	4	Late Cretaceous
Propsector Mountain (felsic)	LKfxPp	5.97	0.14	0.03	19.40	9.39	11	
Carmacks basalt	uKC1	10.71	10.70	8.01	15.10	2.41	8	
Carmacks felsic volcanic	uKC3	0.33	0.14	0.08	0.97	0.42	4	
Casino microdiorite	LKmC	20.87	18.95	8.19	50.70	10.13	16	
Casino felsic	LKfCp	0.12	0.05	0.04	0.32	0.14	4	
Whitehorse Pl porphyry	mKaW	19.56	23.80	4.58	30.30	13.37	3	mid-Cretaceous
Whitehorse granodiorite	mKgWT	13.22	11.10	0.13	32.80	10.18	24	
Whitehorse Qz porphyry	mKfWp	1.04	0.45	0.02	3.81	1.25	15	
Mount Nansen (felsic)	mKNFt, mKNFf	0.04	0.05	0.00	0.08	0.03	5	
Mount Nansen (intermediate)	mKNAm, mKNAb	17.10	14.60	0.09	55.80	14.09	52	
Minto	LTrEJgM, LTrEJgM1	8.25	6.18	0.09	26.00	6.91	56	metamorphic basement
Pyroxene Mountain	LTrPx	0.26	0.26	0.12	0.41	0.20	2	
Sulphur Creek	PgS	0.19	0.03	0.01	0.53	0.30	3	
Simpson Range	MgSR	1.51	0.31	0.00	10.90	2.95	13	
Finlayson amphibolite	DMF1	0.67	0.21	0.04	2.93	0.87	11	
Snowcap amphibolite	PDS3	9.27	4.09	0.11	24.00	11.12	6	
Snowcap schist	PDS1	1.69	0.32	0.01	18.10	3.88	33	

Minto suite (LTrEJgM)

Plutons of the Minto suite are relatively widespread in the central part of the Mount Nansen area (Fig. 2). Two textural varieties are recognized, a K-feldspar porphyritic hornblende granodiorite and an equigranular hornblende granodiorite (Sack *et al.*, 2021). Both phases are medium to coarse grained and moderately foliated to unfoliated; foliation intensity tends to increase on the eastern side of plutons (Sack *et al.*, 2021). We report an emplacement age for the Victoria Creek pluton of *ca.* 199 Ma, similar to other Minto suite plutons to the north and northeast that range from 205 to 194 Ma (Sack *et al.*, 2020). The magnetic susceptibility of the Minto plutonic suite ranges from 26.0 to 0.09 × 10³ SI units with a median value of 6.18 (Table 1).

Long Lake suite (EJyL)

In the Mount Nansen area, Long Lake suite rocks are only recognized near Seymour Creek at the north edge of the map (Allan and Friend, 2018). Here the Long Lake suite comprises a composite batholith, the phase that is mapped locally is very coarse grained, crowded K-feldspar porphyritic hornblende monzonite to syenite; K-feldspar phenocrysts are up to 5 cm (Carlson, 1987). This alkalic phase of the batholith was emplace *ca.* 185 Ma (Sack *et al.*, 2020).

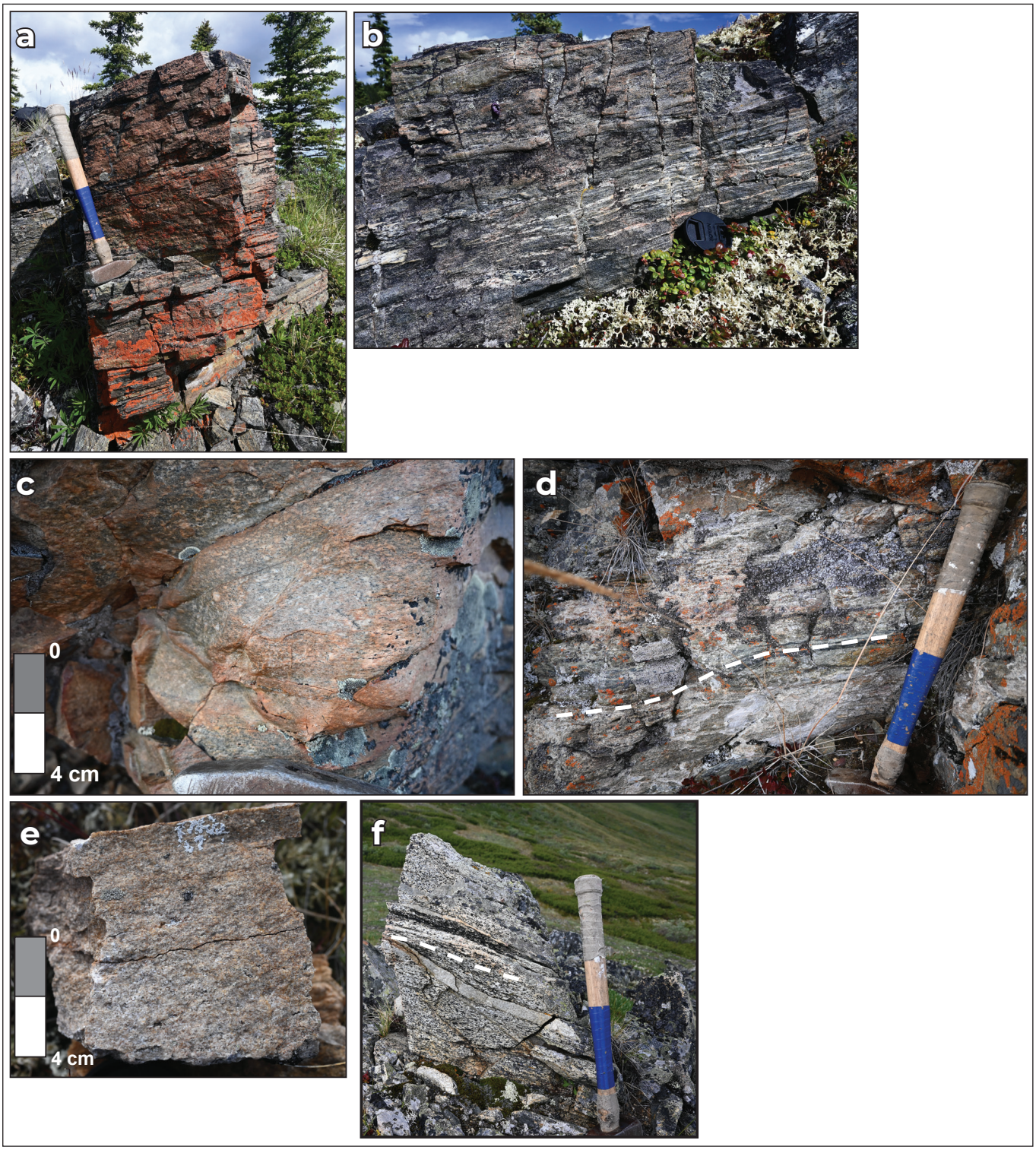

Figure 3. *Representative photos of metamorphic basement rocks in the Mount Nansen area.* **(a)** *20PS017, weathered outcrop of quartz-mica schist, the main lithology of the Snowcap assemblage in the Mount Nansen area. Hammer is 45 cm long.* **(b)** *20PS021, foliated amphibolite within the Snowcap assemblage.* **(c)** *20PS217, plagioclase augen gneiss of the Simpson Range suite.* **(d)** *20PS214, foliated amphibolite of the Finlayson assemblage. Dashed white line shows main foliation trace. Hammer is 45 cm long.* **(e)** *20PS102, fine to medium-grained, sugary metaplutonic rock of the Sulphur Creek suite.* **(f)** *20PS050, foliated, medium-grained granodiorite of the Minto suite crosscut by thin, unfoliated aplite dikes. Dashed white line shows main foliation trace. Hammer is 45 cm long.*

Mid-Cretaceous igneous rocks

Mid-Cretaceous volcanic and plutonic rocks are primarily found in the central and western parts of the Mount Nansen area (Fig. 2) and comprise a volcano-plutonic complex formed ca. 115 to 105 Ma (Klöcking et al., 2016; Ryan et al., 2016; Sack et al., 2021). The magnetic susceptibility of these rocks varies over three orders of magnitude (Table 1) but in general, these rocks have relatively high magnetic susceptibility and are mostly magnetic highs on regional aeromagnetic maps (Aurora Geosciences and Bruce, 2020).

Mount Nansen group

Volcanic rocks of the Mount Nansen group are primarily found in the central part of the area on Mount Nansen and Victoria Mountain (Fig. 2). Intermediate and felsic rocks of the Mount Nansen group are broadly coeval with crystallization ages ca. 115 to 107 Ma (Klöcking et al., 2016).

Intermediate volcanic rocks (mKNA)

The bulk of the Mount Nansen group is andesitic in composition with textural varieties that include massive, plagioclase-phyric flows, monomictic autobreccias and lesser rounded, polymictic breccias (Fig. 4). The magnetic susceptibility of the intermediate Mount Nansen rocks ranges from 55.8 to 0.09 × 10³ SI units with a median value of 14.6 (Table 1). All andesitic varieties are dark green to brown weathered and dark green to black fresh. In massive andesite, 2–5 mm white plagioclase phenocrysts give a speckled appearance (Fig. 4a).

Figure 4. *Representative photos of mid-Cretaceous volcanic rocks in the Mount Nansen area.* ***(a)*** *20PS143, weathered outcrop of massive, plagioclase phyric andesite, the most widespread lithology of the Mount Nansen group in the map area.* ***(b)*** *20PS105, volcanic, matrix supported conglomerate of primarily andesitic cobbles within an andesitic matrix. Hammer head is 13 cm.* ***(c)*** *20PS142, flow banded rhyolite of the Mount Nansen group. Scribe for scale.*

Felsic volcanic rocks (mKNF)

Felsic volcanic rocks within the Mount Nansen group are relatively rare, occurring as local flows and domes, mostly in the upper part of the stratigraphy preserved near the top of Mount Nansen (Klöcking *et al.*, 2016). These rocks are rhyolitic in composition and range from aphanitic densely welded tuff to autoclastic rhyolite breccia and flow-banded rhyolite (Fig. 4c). They are light grey to buff, weathered and fresh. The magnetic susceptibility of the felsic Mount Nansen rocks ranges from 0.08 to 0.0043 × 10³ SI units with a median value of 0.05 (Table 1).

Whitehorse suite

Porphyry plugs and dikes (mKfWp)

Small plugs and dikes associated with the main Dawson Range granodiorite phase of the Mount Nansen pluton are found throughout the Mount Nansen area (Fig. 2). The dikes are typically small, up to metres across, and porphyritic with two phenocryst assemblages: plagioclase only and quartz-plagioclase. The plagioclase only porphyries are relatively rare. They are dull grey-brown on weathered and fresh surfaces and friable. The plagioclase phenocrysts commonly have a radiating texture giving the rock a 'flower' porphyry appearance. The magnetic susceptibility of Whitehorse suite plagioclase porphyritic dikes ranges from 30.3 to 4.58 × 10³ SI units with a median value of 23.8 (Table 1).

The quartz-plagioclase porphyries are more volumetrically and economically significant and the largest of these bodies is the plug on Dickson Hill immediately north of the Flex deposit (115I 137). These dikes and plugs have rhyolitic to dacitic compositions and are light grey to orange-weathered and light grey fresh. The phenocryst assemblage has plagioclase > quartz with white subround 2–3 mm plagioclase crystals and clear 3–5 mm, angular to subround quartz crystals that are commonly embayed (Fig. 5a). The magnetic susceptibility of Whitehorse suite quartz-feldspar porphyritic dikes ranges from 3.81 to 0.02 × 10³ SI units with a median value of 0.45 (Table 1). These rocks were previously interpreted as Late Cretaceous (Sack *et al.*, 2021) however, they are now known to be mid-Cretaceous as the crystallization age of the Dickson Hill plug is 111 ± 1.8 Ma (this study).

Granodiorite (mKfW)

The main phase of the Whitehorse suite, also known as the Dawson Range granodiorite (Ryan *et al.*, 2016), in the Mount Nansen area is a fine to medium-grained, equigranular biotite-hornblende granodiorite of the Mount Nansen pluton (Fig. 6a; Sack *et al.*, 2021). The Mount Nansen pluton and associated dikes are *ca.* 107 to 105 Ma (Klöcking *et al.*, 2016; Mortensen *et al.*, 2016; this study). The magnetic susceptibility of Whitehorse suite granodiorite and granite ranges from 32.8 to 0.13 × 10³ SI units with a median value of 11.1 (Table 1).

Granite (mKaW)

The other volumetrically significant phase of the Mount Nansen pluton is the Bow Creek granite (Carlson, 1987). This phase is predominantly recognized in the headwaters of Bow Creek near the north edge of the Mount Nansen area (Fig. 2), though small dikes are recognized on the flanks of Mount Nansen as well (Klöcking *et al.*, 2016). The Bow Creek granite is a zoned pluton with a core of fine-grained equigranular, biotite ± hornblende granite and a border phase of quartz-plagioclase-biotite porphyritic granite. Both phases are pink on weathered and fresh surfaces (Fig. 6b,c). The crystallization age of both phases is *ca.* 108 Ma with the core slightly older than the border phase (this study).

Late Cretaceous igneous rocks

Casino plugs and dikes (LKC)

There are felsic and mafic Casino age (*ca.* 78 to 74 Ma) dikes and plugs in the Mount Nansen area. The felsic variety are found as dikes and are best understood in the vicinity of the Klaza deposit (15I 067). These dikes are feldspar > quartz porphyritic granodiorite with very fine grained biotite in the groundmass (Lee *et al.*, 2020). The dikes are commonly co-spatial with, and cut by, composite epithermal veins of the Klaza deposit (Lee *et al.*, 2020). The phenocryst assemblage and composition of these dikes is very similar to the mid-Cretaceous plugs and dikes, and differentiating them in the field is difficult. The age of these dikes in the vicinity of the Klaza deposit is 78 to 76 Ma (Lee, 2021).

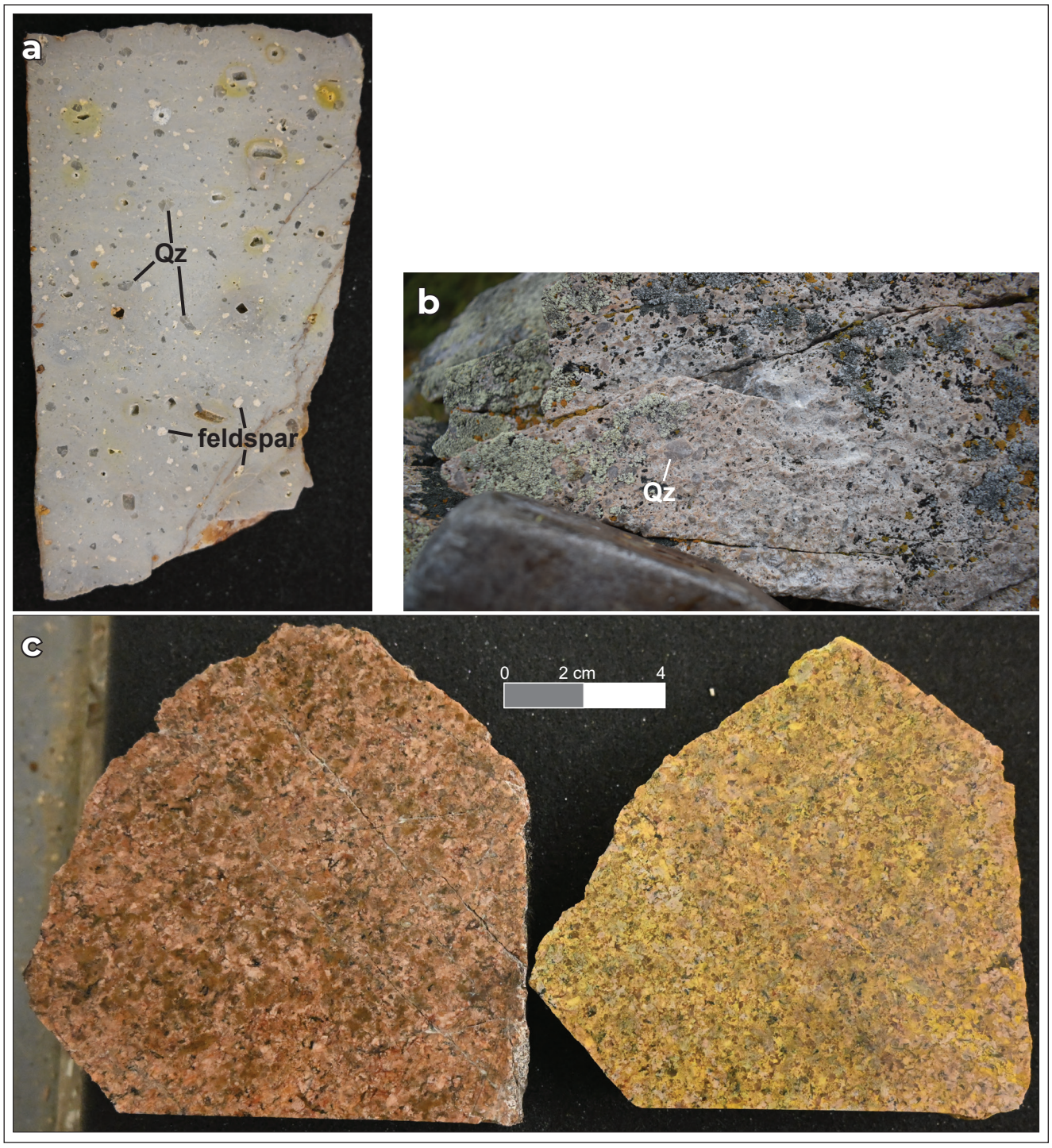

Figure 5. *Representative photos of mid-Cretaceous plutonic rocks in the Mount Nansen area analyzed for U-Pb zircon dating at Boise State University.* ***(a)*** *20PS218-1, cobaltinitrite stained slab of silica and clay altered quartz-plagioclase porphyritic rock from Dickson hill; 111 Ma. Slight yellow stain of feldspars indicate they are plagioclase.* ***(b)*** *20PS190-1, outcrop of quartz-feldspar porphyritic granite from the central phase of the Bow Creek pluton; 107.86 Ma.* ***(c)*** *20PS194-1, polished (L) and sodium cobaltinitrite stained (R) slabs of the border phase of the Bow Creek pluton, same phase as 20PS195-1 which has been dated in this study at 107.96 Ma. All photos are the same scale.*

Figure 6. *Representative photos of plutonic rocks in the Mount Nansen area analyzed for U-Pb zircon dating at Memorial University.* **(a)** *2010vb0046, medium-grained hornblende-biotite granodiorite of the Dawson Range batholith, country rock to the Klaza deposit; 107.0 Ma.* **(b)** *2010vb0047, mineralized feldspar porphyritic dike crosscutting the Dawson Range batholith at the Klaza deposit.* **(c)** *2010vb0055, deformed K-feldspar porphyritic hornblende granodiorite of the Minto suite, country rock to the Brown-McDade deposit.* **(d)** *2010vb0056, brecciated feldspar porphyritic dike crosscutting Minto suite granodiorite at the Brown-McDade pit. Centimetre graduations on scale card in each photo.*

More voluminous throughout the Mount Nansen area are a series of small, equigranular, hornblende ± pyroxene microdiorite plugs (Fig. 7a). The best exposure of this unit is in the vicinity of Slate Creek immediately south of the Klaza deposit (Fig. 2). The unit was originally recognized in early mapping (Sawyer and Dickinson, 1976) but was thought to be related to mid-Cretaceous magmatism (Sack *et al.*, 2021). Sack *et al.*, 2022 report a *ca.* 78 Ma age for the Kelly plug confirming it is coeval with the Casino suite and is likely related to the Kelly porphyry system (115I 156, 157) as Sack *et al.*, 2022 report Re-Os molybdenite ages between 81 and 76 Ma. The magnetic susceptibility of Casino suite dikes ranges from 0.32 to 0.04 × 10³ SI units with a median value of 0.05, the microdiorite plugs range from 50.7 to 18.9 × 10³ SI units with a median value of 18.95 (Table 1).

Carmacks group

The Carmacks group volcanic rocks are the youngest widespread rocks in the Mount Nansen area and are primarily preserved in the northeastern part of the area (Fig. 2). A crude stratigraphy is recognized in the Mount Nansen area with a basal felsic unit overlain by a lower andesite and capped by upper basalt flows, the most regionally extensive unit (Carlson, 1987). In the Mount Nansen area, this stratigraphy can be seen on the south side of Rowlinson Creek and the headwaters of Bow Creek (Fig. 2). Based on K-Ar and Ar-Ar dates outside the Mount Nansen area, Carmacks group rocks were deposited between 73 and 68 Ma (Grond *et al.*, 1984; Joyce *et al.*, 2015).

Felsic volcanic rocks (LKfC)

The basal felsic unit is an alkalic rhyolite crystal tuff with 5–10% quartz and feldspar shards, and 1–2% tabular biotite. The unit is flaggy, weathers pale pink and is light grey on fresh surfaces. The groundmass is very fine grained and potassic (Fig. 7b,c). The magnetic susceptibility of Carmacks group felsic rocks ranges from 0.97 to 0.08 × 10³ SI units with a median value of 0.14 (Table 1).

Intermediate volcanic rocks (uKC)

The lower andesitic rocks outcrop on the margins of the basalt unit and are primarily tuff and volcanic breccia with a phenocryst assemblage of plagioclase, hornblende and rarely pyroxene (Carlson, 1987). These rocks typically weather pink to red to reddish-brown and are grey to green on fresh surfaces (Carlson, 1987).

Mafic volcanic rocks (uKC)

These are the most regionally extensive rocks in the Carmacks group (Ryan *et al.*, 2013, 2016) and are pyroxene ± olivine porphyritic basalt flows that weather dark red to brown and are dark green on fresh surfaces (Fig. 7d). The magnetic susceptibility of Carmacks group basalt ranges from 15.1 to 8.01 × 10³ SI units with a median value of 10.7 (Table 1).

Prospector Mountain suite

Felsic plutonic rocks (LKfxPp)

Felsic rocks of Prospector Mountain suite age (72 to 68 Ma) are primarily found near the Cyprus porphyry body near the East Fork of Nansen Creek (Fig. 2). The Cyprus porphyry is an intrusive breccia complex with light grey to orange-weathered, heterolithic, clast-supported breccia containing subangular to rounded sand to pebble-sized clasts of light grey porphyritic rock in a fine-grained cream to pink matrix. It is locally quartz-sericite-pyrite altered (Sawyer and Dickinson, 1976). Porphyry mineralization is associated with the Cyprus porphyry and includes chalcopyrite-pyrite ± molybdenite stockwork veining at *ca.* 71 Ma (Selby *and Creaser,* 2001; Lee, 2021). The magnetic susceptibility of felsic Prospector Mountain rocks ranges from 19.4 to 0.03 × 10³ SI units with a median value of 0.14 (Table 1).

Mafic plutonic rocks (LKdP)

Mafic plutonic rocks of the Prospector Mountain suite are pyroxene ± biotite porphyritic monzodiorite to monzogabbro. They are brown to black on weathered and fresh surfaces and are massive, medium grained and melanocratic with an alkali groundmass (Fig. 7e,f). These plugs are best recognized south of Rowlinson Creek where they intrude Carmacks group basalt (Fig. 2).

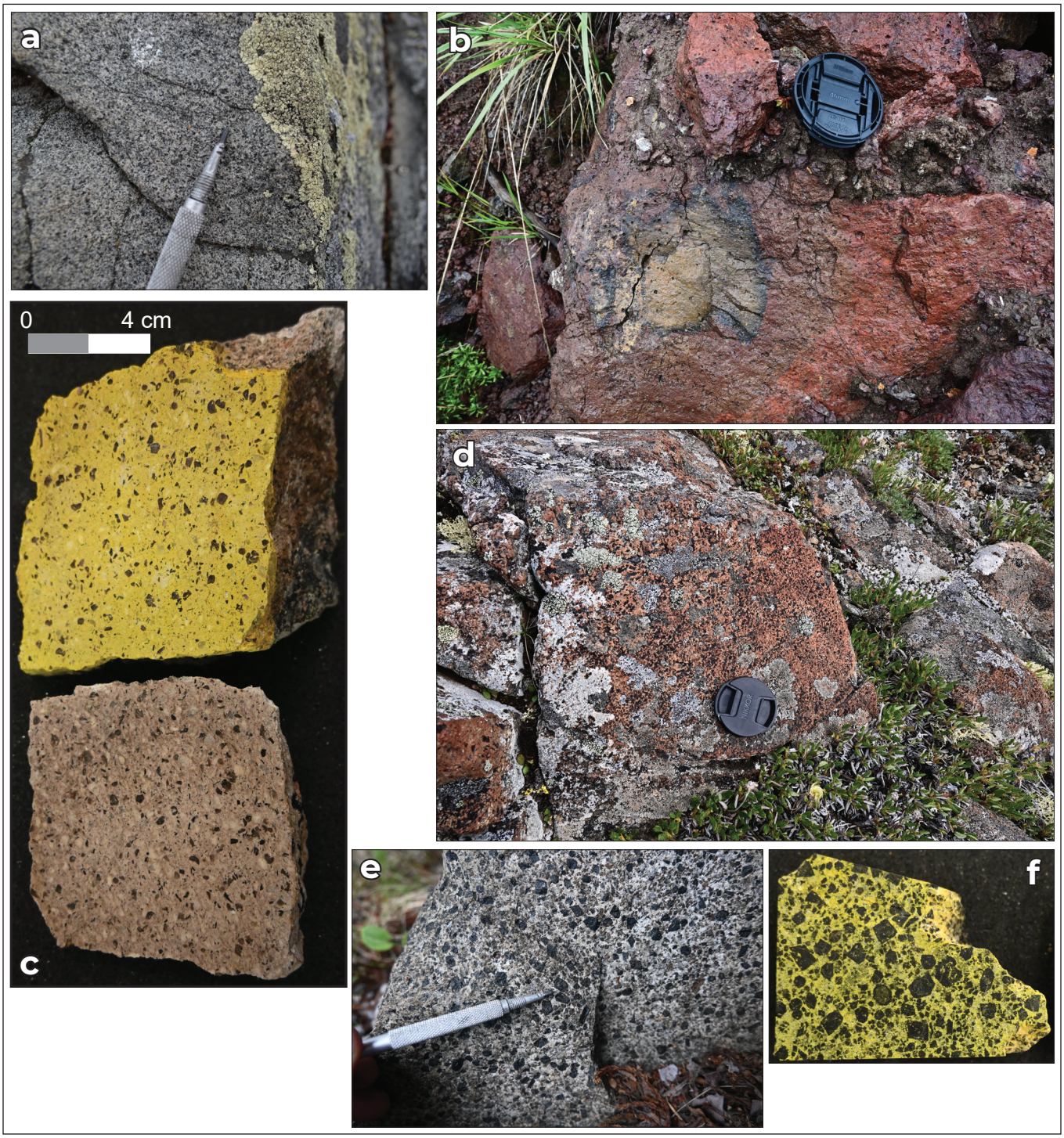

Figure 7. *Representative photos of Late Cretaceous rocks in the Mount Nansen area.* ***(a)*** *19PS046, weathered surface of microdiorite from the Kelly plug; this body has a crystallization age of 78.11 ± 0.03 Ma (Sack et al., 2022). Scribe for scale.* ***(b)*** *20PS004, weathered outcrop of intermediate to felsic volcanic breccia near the base of the Carmacks Group. Lens cap is 5 cm in diameter.* ***(c)*** *20PS161-1, sodium cobaltinitrite stained (upper) and polished (lower) slabs of alkalic crystal tuff from the lower Carmacks Group.* ***(d)*** *20PS024, red-brown weathered outcrop of olivine-pyroxene basalt from the upper (main) Carmacks Group. Lens cap is 5 cm in diameter.* ***(e)*** *20PS002, coarse-grained pyroxene-phyric gabbro that intrudes basalt of the Carmacks Group. Scribe for scale.* ***(f)*** *20PS002-1, sodium cobaltinitrite stained slab of coarse-grained pyroxene-phyric gabbro showing the alkalic nature (yellow) of the groundmass. Same scale as* ***(c)***.

The magnetic susceptibility of mafic Prospector Mountain rocks ranges from 20.7 to 0.2 × 10³ SI units with a median value of 6.49 (Table 1). These rocks are equivalent to unit uKCg of Colpron et *al.* (2007) 60 km to the east where they have a biotite K-Ar cooling age of *ca.* 68 Ma (Grond et *al.*, 1984), an age which is consistent with these plugs locally intruding Carmacks group basalt.

Paleogene igneous rocks

Rhyolite Creek dikes (PRc)

Rhyolite Creek rocks are more commonly recognized to the west of the Mount Nansen area, but porphyritic, tan to cream, locally flow banded, rhyolite dikes and sills with smoky quartz ± feldspar phenocrysts are mapped along the western part of the area (Ryan et *al.*, 2016). These rocks are *ca.* 58 Ma (Ryan et *al.*, 2016).

Methods

U-Pb zircon geochronology

Boise State University

Three mid-Cretaceous plutonic samples underwent U-Pb zircon geochronological analysis at Boise State University using a method similar to that described in Sack et *al.* (2020). This method includes reconnaissance laser ablation-inductively coupled plasma mass spectrometer (LA-ICPMS) analyses of a relatively large number of crystals per sample (up to 51 in this study) to characterize zircon populations followed by chemical abrasion-thermal ionization mass spectrometry (CA-TIMS) analysis of 5 or 6 crystals from the youngest coherent population. Appendix 2 includes a detailed description of the analytical method, cathodoluminescence (CL) images of zircon with located laser spots, as well as results of LA-ICPMS

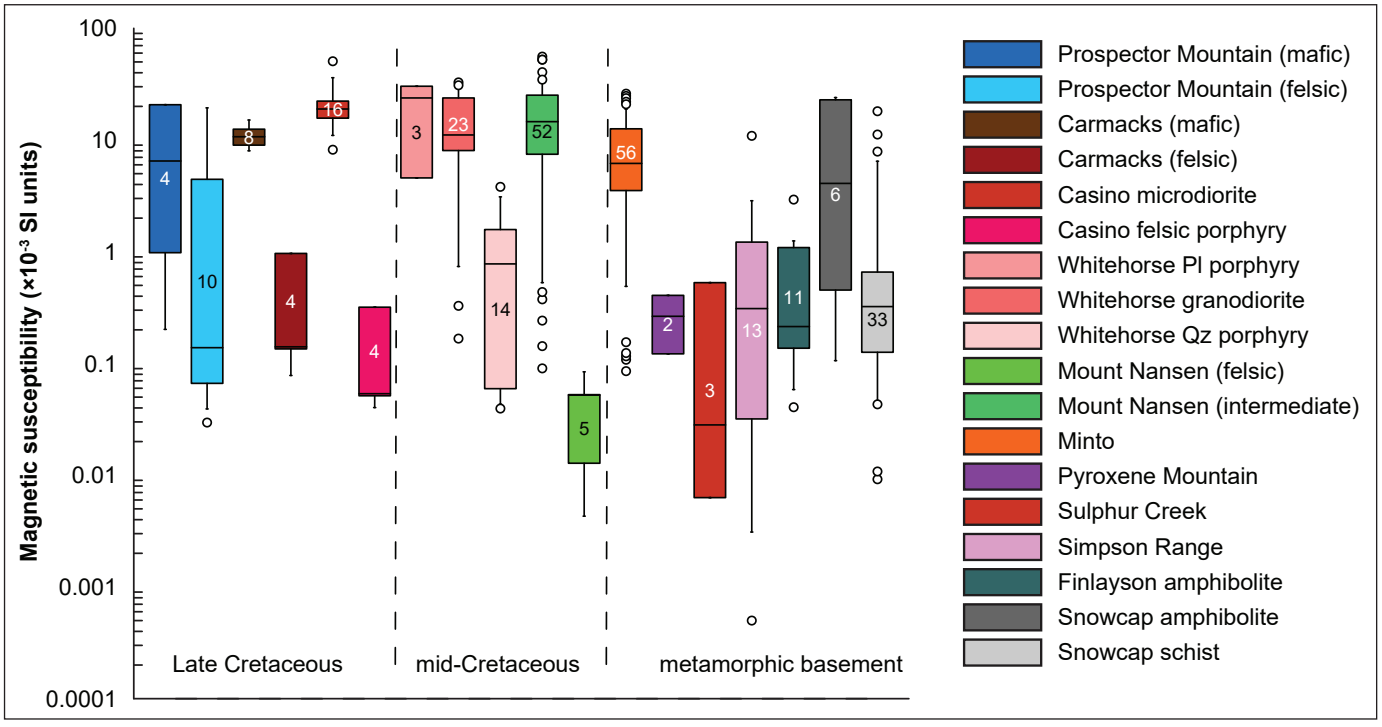

Figure 8. *Box-whisker plot of magnetic susceptibility data for rocks in the Mount Nansen area. Data in Appendix 1 and summarized in Table 1. Whiskers are 10th and 90th percentile, box edges are 25th and 75th percentile and centre line within box is median of data; small white circles represent outlier data. Number within each box is the number of stations with data. Magnetic susceptibility at each station is the average of five measurements over a 1 to 2 m² area within the same lithology.*

and CA-TIMS analyses. For two samples, we use the more precise weighted mean date of CA-TIMS analyses to determine the crystallization age of samples. For sample 19PS004-1, only nine crystals were recovered during separation and only LA-ICPMS analyses were conducted; for this sample the weighted mean date of LA-ICPMS data is used to determine the crystallization age. All errors are reported at 2σ.

Memorial University

Five plutonic samples underwent U-Pb zircon geochronological analysis at Memorial University following the method described by Bennett and Tubrett (2010). This is a LA-ICPMS method that utilizes line ablation with a 10 µm or 20 µm spot size and ablation of either a 40 µm by 40 µm raster or a line. Backscatter electron (BSE) images of zircon crystals were used to locate homogeneous zones for ablation. Results of LA-ICPMS analysis are included in Appendix 2; representative BSE images of zircon are shown in Figures 12 to 16. All errors are reported at 2σ.

Pb isotope geochemistry

The lead isotopic composition of feldspar from igneous rocks was determined at the Pacific Centre for Isotopic and Geochemical Research at the University of British Columbia. Feldspar separates were washed and dissolved in dilute hydrochloric acid, then prepared and analyzed using the TIMS method described by Mortensen and Gabites (2002). Errors are reported at 2σ. Data are in Table 4.

Results

Geochronology

Table 2 summarizes the new geochronological results for the Mount Nansen area.

Sample 20PS190-1 is a quartz-feldspar porphyritic granite collected from Bow Creek pluton (unit 8c of Carlson, 1987; Fig. 2). It yielded euhedral, concentrically zoned zircons with 2:1 aspect ratios (Fig. 9a).

Table 2. *Summary table of geochronology results.*

Sample	Latitude	Longitude	Pluton/ Location	Lithology	Method	Weighted mean $^{206}Pb/^{238}U$ date (Ma)	± 2δ (Ma)	total n	n in weighted mean	MSWD	pof	Inheritance
20PS190-1	62.156839	-137.252990	Bow Creek	quartz-feldspar porphyritic granite	CA-TIMS	107.86	0.03	5	5	0.80	0.53	none
20PS195-1	62.176095	-137.282900	Bow Creek	biotite granite	CA-TIMS	107.96	0.03	6	6	1.20	0.29	none
19PS004-1	62.053260	-136.167480	Flex knob	quartz-feldspar porphyry	LA-ICPMS	111.00	1.8	7	6	1.02	0.40	1 @ 344 Ma
2010vb0045	62.127500	-137.247167	Klaza trench 09	mineralized feldspar porphyry dike	LA-ICPMS	107.00	0.72	20	20	0.59	0.92	none
2010vb0046	62.127361	-137.247305	Klaza trench 09	hornblende-biotite granodiorite	LA-ICPMS	107.00	0.78	20	20	0.55	0.94	none
2010vb0047	62.117528	-137.248972	Klaza trench 02?	mineralized feldspar porphyry dike	LA-ICPMS	107.50	0.67	25	25	0.39	1.00	none
2010vb0055	62.051444	-137.126167	Brown-McDade pit	deformed hornblende-biotite granodiorite	LA-ICPMS	199.06	0.96	24	23	3.55	0.00	1 @ 340 Ma
2010vb0056	62.051444	-137.126167	Brown-McDade pit	brecciated feldspar porphyry dike	LA-ICPMS	198.74*	1.18	24	21	3.82	0.00	1 @ 76, 1 @ 106 Ma

* calculations for population of Early Jurassic dates from crystals interpreted as inherited

Fifty-one LA-ICPMS spot analyses yielded $^{206}Pb/^{238}U$ dates between 109 and 101 Ma. The weighted mean of all 51 LA-ICPMS dates is 105.53 ± 0.51 Ma (n = 51 of 51; Fig. 9b). Five zircons from 20PS190-1 were analyzed by CA-TIMS and yielded equivalent $^{206}Pb/^{238}U$ dates ranging from 107.90 ± 0.08 to 107.81 ± 0.08 Ma (Table 2), with a weighted mean age of 107.86 ± 0.03 Ma (MSWD = 0.8, n = 5; Fig. 9c; Table 2). This is the best estimate of the crystallization age for this phase of the Bow Creek pluton.

Sample 20PS195-1 is a quartz-feldspar porphyritic biotite granite collected from Bow Creek pluton (unit 8b of Carlson, 1987; Fig. 2). It yielded euhedral, concentrically zoned zircons with 2:1 aspect ratios (Fig. 10a). Thirty-three LA-ICPMS spot analyses yielded $^{206}Pb/^{238}U$ dates between 113 and 100 Ma. The weighted mean of all 33 LA-ICPMS dates is 104.74 ± 0.60 Ma (n = 33 of 33; Fig. 10b). Six zircons from 20PS195-1 were analyzed by CA-TIMS and yielded equivalent $^{206}Pb/^{238}U$ dates ranging from 108.02 ± 0.07 to 107.91 ± 0.07 (Table 3), with a weighted mean age of 107.96 ± 0.03 Ma (MSWD = 1.2, n = 6; Fig. 10c; Table 2). This is the best estimate of the crystallization age for this phase of the Bow Creek pluton.

Sample 19PS004-1 is a clay altered quartz-feldspar porphyry collected from north end of the Flex deposit and is interpreted to be part of the Dickson plug (Fig. 2). This sample yielded nine subhedral to euhedral, sector

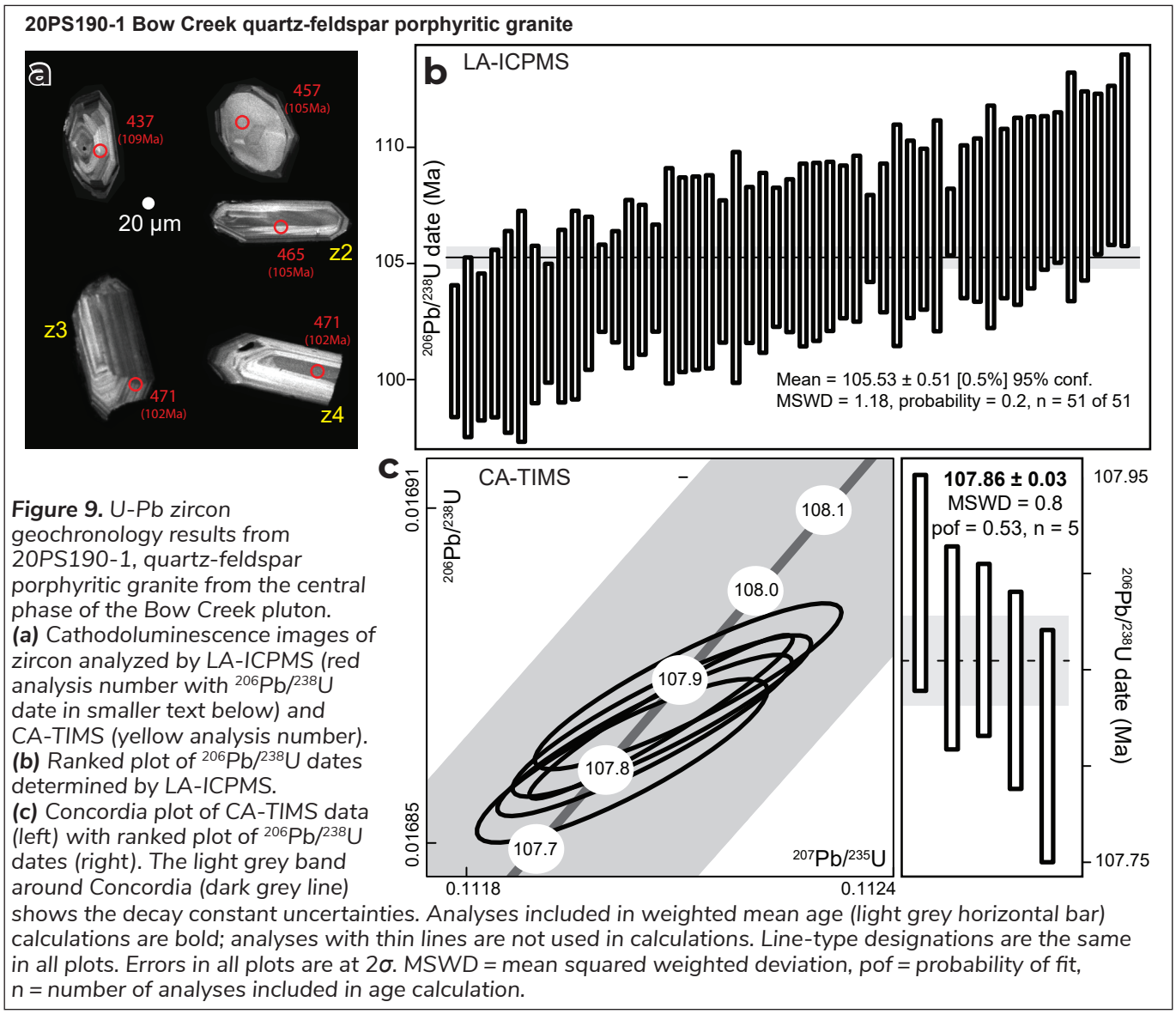

Figure 9. *U-Pb zircon geochronology results from 20PS190-1, quartz-feldspar porphyritic granite from the central phase of the Bow Creek pluton.* ***(a)*** *Cathodoluminescence images of zircon analyzed by LA-ICPMS (red analysis number with $^{206}Pb/^{238}U$ date in smaller text below) and CA-TIMS (yellow analysis number).* ***(b)*** *Ranked plot of $^{206}Pb/^{238}U$ dates determined by LA-ICPMS.* ***(c)*** *Concordia plot of CA-TIMS data (left) with ranked plot of $^{206}Pb/^{238}U$ dates (right). The light grey band around Concordia (dark grey line) shows the decay constant uncertainties. Analyses included in weighted mean age (light grey horizontal bar) calculations are bold; analyses with thin lines are not used in calculations. Line-type designations are the same in all plots. Errors in all plots are at 2σ. MSWD = mean squared weighted deviation, pof = probability of fit, n = number of analyses included in age calculation.*

zoned and weakly concentrically zoned zircons with 1:1 to 2:1 aspect ratios (Fig. 11a). Seven LA-ICPMS spot analyses yielded six $^{206}Pb/^{238}U$ dates between 114 and 108 Ma and one inherited grain at 344 Ma. The weighted mean of the six LA-ICPMS dates is 111.00 ± 1.8 Ma (n = 6 of 7; Fig. 11b; Table 2). Due to the low number of zircon crystals recovered, further CA-TIMS analyses were not done. The weighted mean of the LA-ICPMS dates is the best estimate of the crystallization age of the Dickson plug.

Sample 2010vb0045 is a mineralized feldspar porphyry dike collected from trench 9 at the Klaza deposit (Fig. 2). This sample yielded euhedral, sector zoned and concentrically zoned zircons with 1:1 to 2:1 aspect ratios and bright rims (Fig. 12a). Twenty LA-ICPMS spot analyses yielded $^{206}Pb/^{238}U$ dates between 110 and 103 Ma. The weighted mean of all 20 LA-ICPMS dates is 107.06 ± 0.73 Ma (n = 20 of 20; Fig. 12b; Table 2). The weighted mean of the LA-ICPMS dates is the best estimate of the crystallization age of this dike.

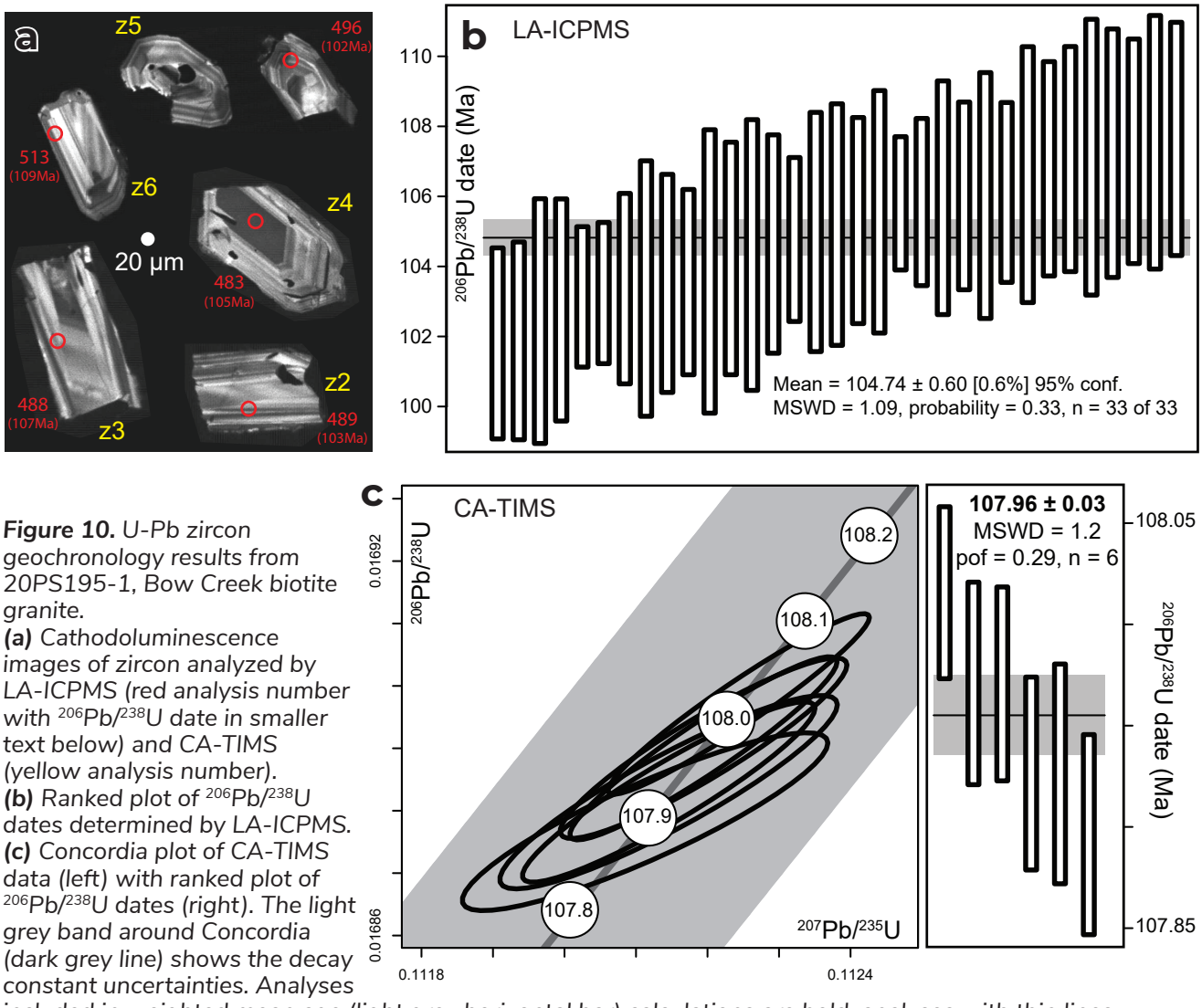

Figure 10. *U-Pb zircon geochronology results from 20PS195-1, Bow Creek biotite granite.*
(a) *Cathodoluminescence images of zircon analyzed by LA-ICPMS (red analysis number with $^{206}Pb/^{238}U$ date in smaller text below) and CA-TIMS (yellow analysis number).*
(b) *Ranked plot of $^{206}Pb/^{238}U$ dates determined by LA-ICPMS.*
(c) *Concordia plot of CA-TIMS data (left) with ranked plot of $^{206}Pb/^{238}U$ dates (right). The light grey band around Concordia (dark grey line) shows the decay constant uncertainties. Analyses included in weighted mean age (light grey horizontal bar) calculations are bold; analyses with thin lines are not used in calculations. Line-type designations are the same in all plots. Errors in all plots are at 2σ. MSWD = mean squared weighted deviation, pof = probability of fit, n = number of analyses included in age calculation.*

Table 3. *CA-TIMS U-Pb zircon data table. The data and calculations for this table are available in Appendix 2.*

										Radiogenic Isotope Ratios								Isotopic Dates						
Sample (a)	Tracer solution	LA-ICPMS spot label	Th/U (b)	$^{206}Pb^*$ x10^{-13} mol (c)	mol % $^{206}Pb^*$ (c)	Pb* (pg) (c)	Pb_c (pg) (c)	Pb*/Pb_c (c)	$^{206}Pb/^{204}Pb$ (d)	$^{208}Pb/^{206}Pb$ (e)	$^{207}Pb/^{206}Pb$ (e)	% err (f)	$^{207}Pb/^{235}U$ (e)	% err (f)	$^{206}Pb/^{238}U$ (e)	% err (f)	corr. coef.	$^{207}Pb/^{206}Pb$ (g)	± (f)	$^{207}Pb/^{235}U$ (g)	± (f)	$^{206}Pb/^{238}U$ (g)	± (f)	include in weighted mean?
20PS190-1																								
z2	BSU1B	465	0.655	0.9527	99.78%	24.72	0.18	140	8123	0.209	0.048290	0.099	0.112337	0.157	0.016880	0.072	0.890	112.43	2.35	108.10	0.16	107.90	0.08	x
z5	BSU1B	473	0.553	1.6862	99.75%	42.62	0.35	122	7237	0.177	0.048257	0.095	0.112225	0.153	0.016874	0.070	0.900	110.82	2.24	108.00	0.16	107.87	0.08	x
z1	BSU1B	461	0.527	2.0283	99.91%	50.91	0.15	330	19726	0.168	0.048264	0.071	0.112239	0.135	0.016874	0.071	0.953	111.19	1.67	108.01	0.14	107.87	0.08	x
z4	BSU1B	471	0.528	1.3363	99.79%	33.55	0.23	143	8544	0.169	0.048231	0.092	0.112137	0.151	0.016870	0.070	0.910	109.56	2.18	107.92	0.15	107.84	0.07	x
z3	BSU1B	470	0.618	1.8798	99.87%	48.32	0.20	244	14255	0.198	0.048209	0.095	0.112054	0.149	0.016865	0.071	0.863	108.49	2.25	107.84	0.15	107.81	0.08	x
20PS195																								
z4	BSU1B	483	0.913	2.8877	99.92%	79.89	0.18	435	23577	0.292	0.048243	0.069	0.112352	0.133	0.016898	0.070	0.959	110.15	1.64	108.11	0.14	108.02	0.07	x
z2	BSU1B	489	0.892	1.3841	99.85%	38.10	0.18	217	11798	0.285	0.048246	0.086	0.112313	0.146	0.016891	0.070	0.923	110.28	2.03	108.08	0.15	107.98	0.08	x
z1	BSU1B	490	0.905	2.1012	99.91%	58.03	0.15	379	20555	0.289	0.048247	0.073	0.112312	0.136	0.016891	0.071	0.945	110.33	1.73	108.08	0.14	107.98	0.08	x
z3	BSU1B	488	0.871	1.1879	99.83%	32.54	0.17	195	10698	0.279	0.048246	0.088	0.112265	0.149	0.016884	0.070	0.927	110.27	2.08	108.03	0.15	107.93	0.08	x
z6	BSU1B	513	1.095	0.7197	99.78%	20.78	0.13	160	8315	0.350	0.048199	0.109	0.112149	0.172	0.016883	0.075	0.910	108.00	2.57	107.93	0.18	107.93	0.08	x
z5	BSU1B	497	0.905	0.6000	99.72%	16.57	0.14	120	6516	0.289	0.048330	0.129	0.112438	0.186	0.016881	0.069	0.888	114.38	3.04	108.19	0.19	107.91	0.07	x

(a) z1, z2, etc. are labels for analyses composed of single zircon grains that were annealed and chemically abraded (Mattinson, 2005).
(b) Model Th/U ratio calculated from radiogenic $^{208}Pb/^{206}Pb$ ratio and $^{207}Pb/^{235}U$ date.
(c) Pb* and Pbc are radiogenic and common Pb, respectively. mol % $^{206}Pb^*$ is with respect to radiogenic and blank Pb.
(d) Measured ratio corrected for spike and fractionation only. Fractionation correction for analyses done with tracer solution BSU1B is 0.16 ± 0.03 (1 sigma) %/amu (atomic mass unit) for single-collector Daly analyses, based on analysis of EARTHTIME ^{202}Pb-^{205}Pb ET2535 tracer solution. Fractionation correction for analyses done with tracer solution ET2535 is based on measurement of $^{202}Pb/^{205}Pb$ in the tracer solution.
(e) Corrected for fractionation and spike. Common Pb in zircon analyses is assigned to procedural blank with composition of $^{206}Pb/^{204}Pb$ = 18.04 ± 0.61%; $^{207}Pb/^{204}Pb$ = 15.54 ± 0.52%; $^{208}Pb/204Pb$ = 37.69 ± 0.63% (1 sigma). $^{206}Pb/^{238}U$ and $^{207}Pb/^{206}Pb$ ratios corrected for initial disequilibrium in $^{230}Th/^{238}U$ using a D(Th/U) of 0.20 ± 0.05 (1 sigma).
(f) Errors are 2 sigma, propagated using algorithms of Schmitz and Schoene (2007) and Crowley et al. (2007).
(g) Calculations based on the decay constants of Jaffey et al. (1971). $^{206}Pb/^{238}U$ and $^{207}Pb/^{206}Pb$ dates corrected for initial disequilibrium in $^{230}Th/^{238}U$ using a D(Th/U) of 0.20 ± 0.05 (1 sigma).

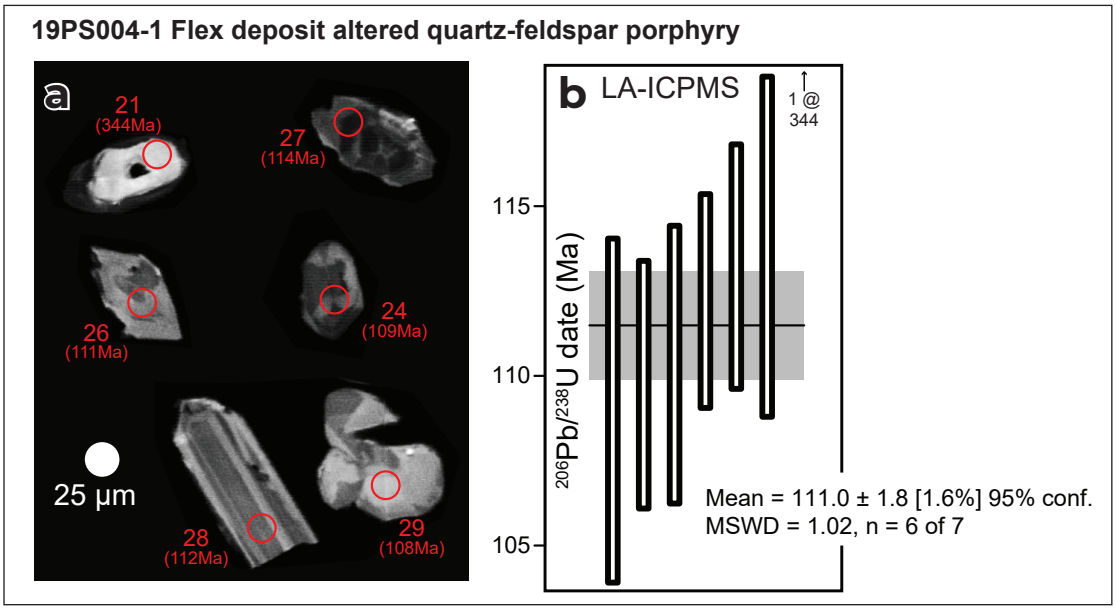

Figure 11. *U-Pb zircon geochronology results from 19PS004-1, Flex plug.* ***(a)*** *Cathodoluminescence images of zircon analyzed by LA-ICPMS (red analysis number with* $^{206}Pb/^{238}U$ *date in smaller text below; open red circle shows approximate location of spot).* ***(b)*** *Ranked plot of* $^{206}Pb/^{238}U$ *dates determined by LA-ICPMS. The light grey band around Concordia (dark grey line) shows the decay constant uncertainties. Analyses included in weighted mean age (light grey horizontal bar) calculations are bold; analyses with thin lines are not used in calculations. Errors are at 2σ. MSWD = mean squared weighted deviation, n = number of analyses included in age calculation.*

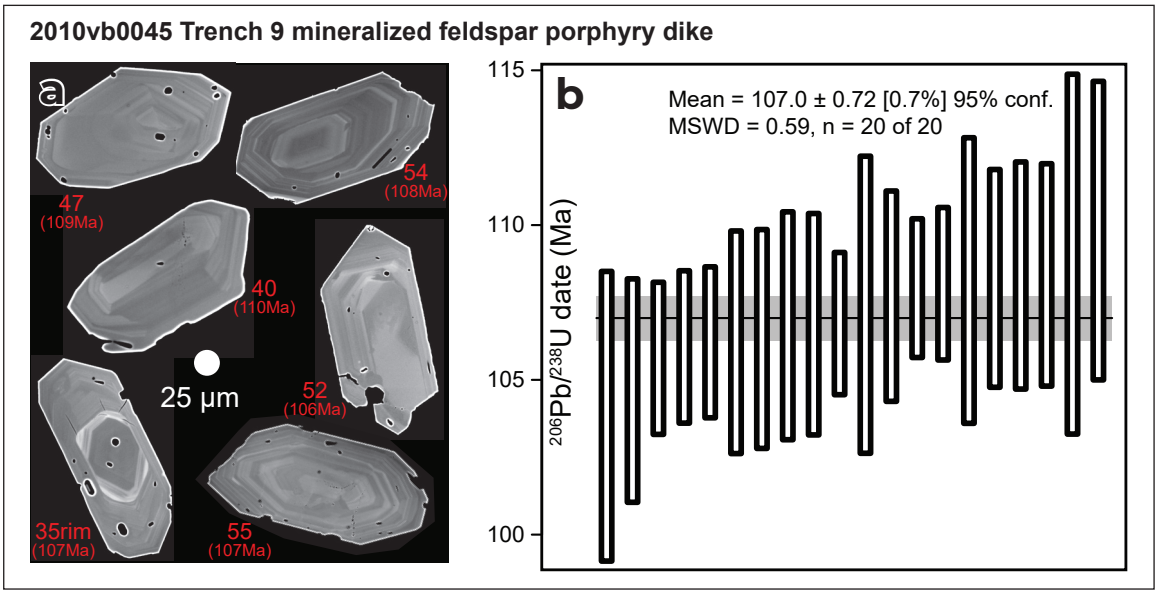

Figure 12. *U-Pb zircon geochronology results from 2010v0045, mineralized feldspar porphyry dike.* ***(a)*** *Backscatter electron (BSE) images of zircon analyzed by LA-ICPMS (red analysis number with 206Pb/238U date in smaller text below).* ***(b)*** *Ranked plot of 206Pb/238U dates determined by LA-ICPMS. The light grey band around Concordia (dark grey line) shows the decay constant uncertainties. Analyses included in weighted mean age (light grey horizontal bar) calculations are bold; analyses with thin lines are not used in calculations. Errors are at 2σ. MSWD = mean squared weighted deviation, n = number of analyses included in age calculation.*

Sample 2010vb0046 is hornblende-biotite granodiorite collected from trench 9 at the Klaza deposit (Fig. 2). It is the country rock to the mineralized feldspar porphyry dike sampled at 2010vb0045 and is part of the Dawson Range batholith. Sample 2010vb0046 yielded euhedral, sector zoned and concentrically zoned zircons with 1:1 to 2:1 aspect ratios and bright rims (Fig. 13a). Twenty LA-ICPMS spot analyses yielded $^{206}Pb/^{238}U$ dates between 109 and 105 Ma. The weighted mean of all 20 LA-ICPMS dates is 107.00 ± 0.78 Ma (n = 20 of 20; Fig. 13b; Table 2). The weighted mean of the LA-ICPMS dates is the best estimate of the crystallization age of this part of the Dawson Range batholith.

Sample 2010vb0047 is a mineralized feldspar porphyry dike collected from trench 2 at the Klaza deposit (Fig. 2). This sample yielded euhedral, sector zoned and concentrically zoned zircons with 1:1 to 2:1 aspect ratios and bright rims (Fig. 14a). Twenty-five LA-ICPMS spot analyses yielded $^{206}Pb/^{238}U$ dates between 110 and 105 Ma. The weighted mean of all 20 LA-ICPMS dates is 107.60 ± 0.71 Ma (n = 25 of 25; Fig. 14b; Table 2). The weighted mean of the LA-ICPMS dates is the best estimate of the crystallization age of this dike.

Sample 2010vb0055 is a foliated hornblende-biotite granodiorite collected from the Brown-McDade pit (Fig. 2). It is the country rock to the mineralized feldspar porphyry dike sampled at 2010vb0056 and is part of the Victoria Creek stock. Sample 2010vb0055 yielded euhedral, sector zoned and concentrically zoned zircons with 1:1 to 4:1 aspect ratios and bright rims (Fig. 15a). Twenty-four LA-ICPMS spot analyses yielded 23 $^{206}Pb/^{238}U$ dates between 215 and 182 Ma and one at 340 Ma. The weighted mean of 19 LA-ICPMS dates is 199.06 ± 0.96 Ma (n = 19 of 24; Fig. 15b; Table 2). The weighted mean of the LA-ICPMS dates is the best estimate of the crystallization age of the Victoria Creek stock.

Sample 2010vb0056 is a mineralized and brecciated feldspar porphyry dike collected from the Brown-McDade pit (Fig. 2). This sample yielded euhedral, sector zoned and concentrically zoned zircons with 1:1 to 2:1 aspect ratios and bright rims (Fig. 16a). Twenty-four LA-ICPMS spot analyses yielded $^{206}Pb/^{238}U$ dates between 213 and 74 Ma. The oldest grain is interpreted as a xenocryst and excluded from age calculations.

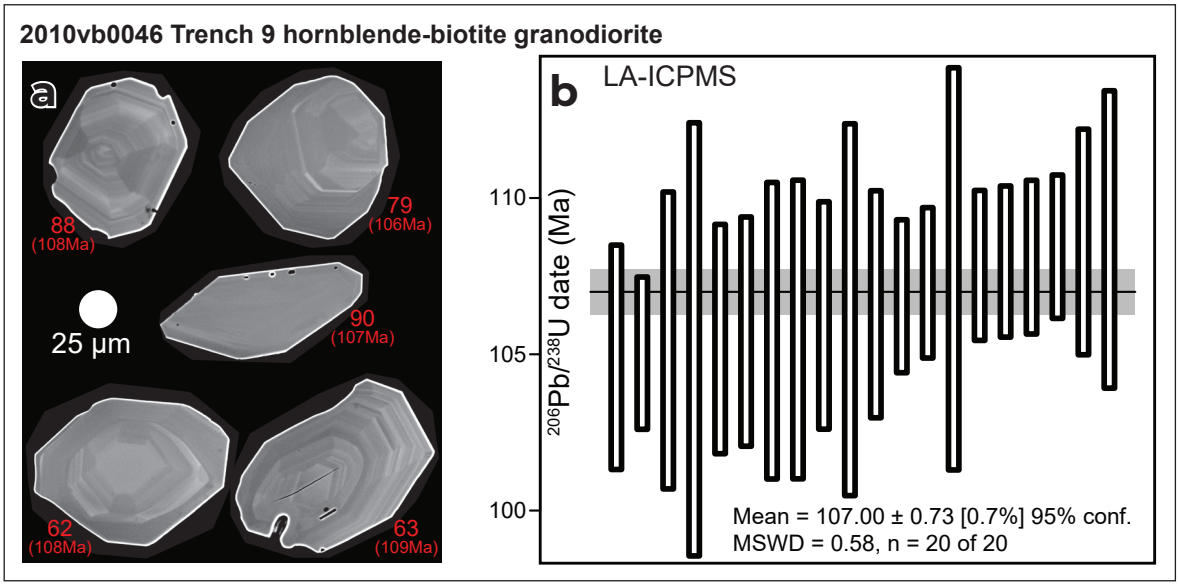

Figure 13. *U-Pb zircon geochronology results from 2010v0046, hornblende-biotite granodiorite.* ***(a)*** *BSE images of zircon analyzed by LA-ICPMS (red analysis number with $^{206}Pb/^{238}U$ date in smaller text below).* ***(b)*** *Ranked plot of $^{206}Pb/^{238}U$ dates determined by LA-ICPMS. The light grey band around Concordia (dark grey line) shows the decay constant uncertainties. Analyses included in weighted mean age (light grey horizontal bar) calculations are bold; analyses with thin lines are not used in calculations. Errors are at 2σ. MSWD = mean squared weighted deviation, n = number of analyses included in age calculation.*

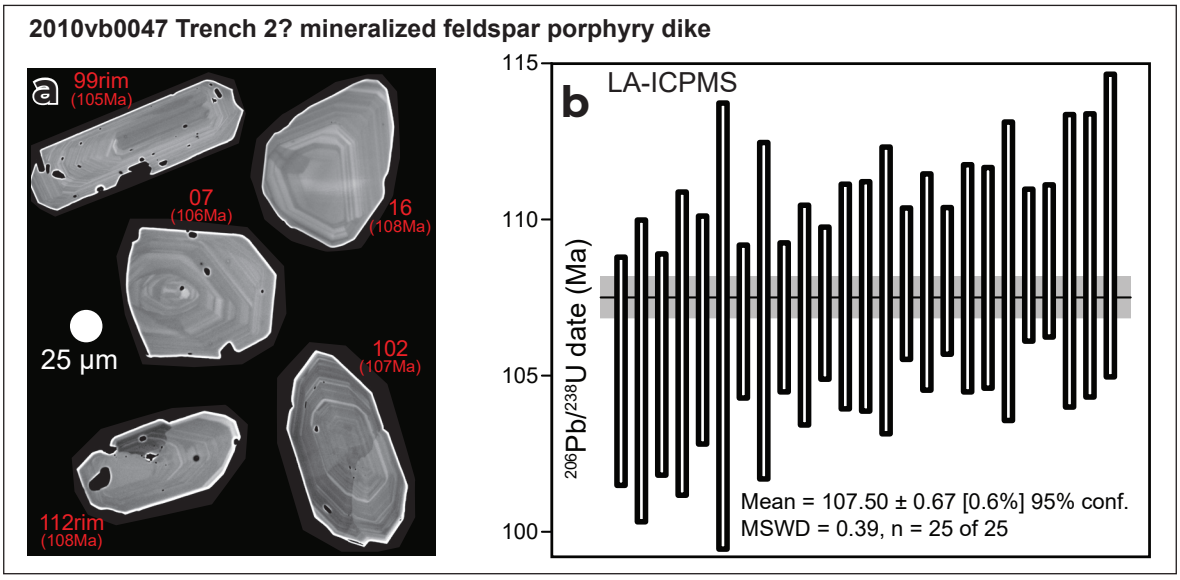

Figure 14. *U-Pb zircon geochronology results from 2010v0047, mineralized feldspar porphyry dike.* **(a)** *BSE images of zircon analyzed by LA-ICPMS (red analysis number with $^{206}Pb/^{238}U$ date in smaller text below).* **(b)** *Ranked plot of $^{206}Pb/^{238}U$ dates determined by LA-ICPMS. The light grey band around Concordia (dark grey line) shows the decay constant uncertainties. Analyses included in weighted mean age (light grey horizontal bar) calculations are bold; analyses with thin lines are not used in calculations. Errors are at 2σ. MSWD = mean squared weighted deviation, n = number of analyses included in age calculation.*

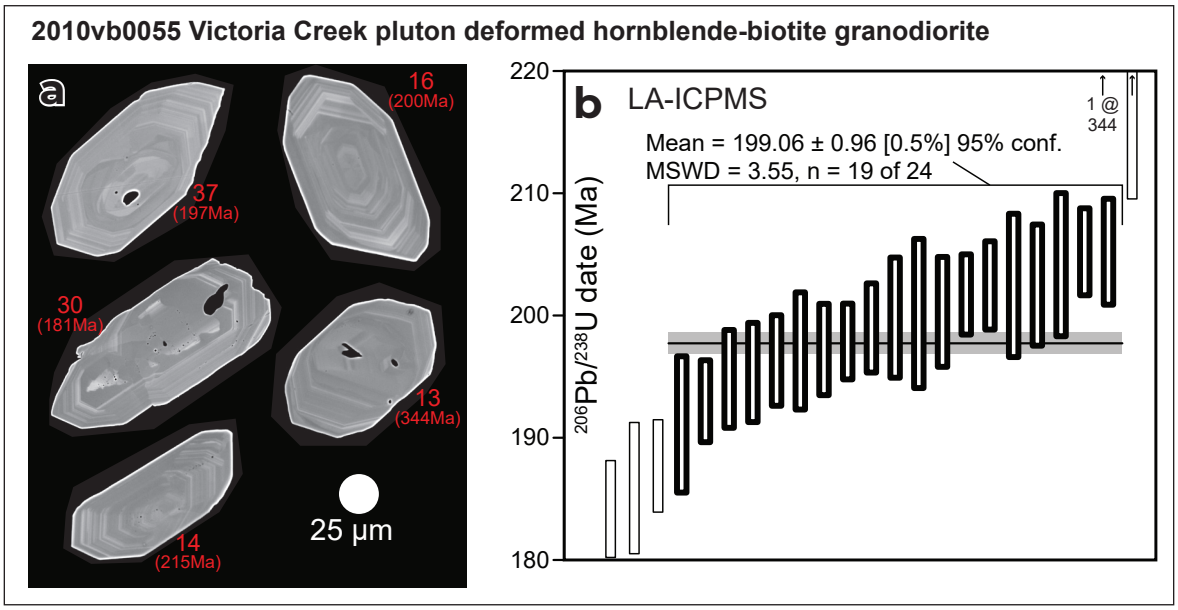

Figure 15. *U-Pb zircon geochronology results from 2010v0055, foliated hornblende-biotite granodiorite from the Brown-McDade pit.* **(a)** *BSE images of zircon analyzed by LA-ICPMS (red analysis number with $^{206}Pb/^{238}U$ date in smaller text below).* **(b)** *Ranked plot of $^{206}Pb/^{238}U$ dates determined by LA-ICPMS. The light grey band around Concordia (dark grey line) shows the decay constant uncertainties. Analyses included in weighted mean age (light grey horizontal bar) calculations are bold; analyses with thin lines are not used in calculations. Errors are at 2σ. MSWD = mean squared weighted deviation, n = number of analyses included in age calculation.*

The significance of two young grains at 106 and 74 Ma is unclear but leaves open the possibility that the dike is as young as Late Cretaceous (ca. 74 Ma). The weighted mean of 21 LA-ICPMS dates is 198.74 ± 1.18 Ma (n = 21 of 24; Fig. 16b; Table 2).The weighted mean of the LA-ICPMS dates is the best estimate of the population of inherited grains that make up the majority of grains recovered from this dike.

Pb isotopes

Radiogenic Pb isotopes ^{206}Pb, ^{207}Pb and ^{208}Pb were analyzed from feldspar from six igneous samples and are reported in Table 4; five samples are plutonic and one is volcanic. Two plutonic samples are Late Triassic to Early Jurassic and the rest of the samples are mid-Cretaceous. The two Late Triassic to Early Jurassic samples have $^{206}Pb/^{204}Pb$ values ranging from 18.960 to 18.846, $^{207}Pb/^{204}Pb$ values ranging from 15.681 to 15.600, and $^{208}Pb/^{204}Pb$ values ranging from 38.859 to 38.548. Sample 20PS218-1 was analyzed three times and is from the mid-Cretaceous Dickson Hill plug (Fig. 2) immediately north of the Flex deposit and has consistently high results with $^{206}Pb/^{204}Pb$ values ranging from 26.800 to 25.825, $^{207}Pb/^{204}Pb$ values ranging from 16.050 to 15.921, and $^{208}Pb/^{204}Pb$ values ranging from 44.474 to 42.139. The remaining three mid-Cretaceous samples, including one duplicate, have $^{206}Pb/^{204}Pb$ values ranging from 19.351 to 19.225, $^{207}Pb/^{204}Pb$ values ranging from 15.728 to 15.634, and $^{208}Pb/^{204}Pb$ values ranging from 39.462 to 38.923.

Discussion

The geology of the Mount Nansen area is presented here using geochronologic evidence to establish the age of events and Pb isotopic evidence to discuss metal sources of mineralizing fluids. For magmatic events, U-Pb zircon are considered the most robust chronometer (closure temperature >700˚C and resistant to subsequent alteration; Hodges, 2014) with CA-TIMS ages the most precise; in a few cases LA-ICPMS ages are the best data available and we use those. For mineralization, Re-Os TIMS ages of molybdenite are considered the best estimate as the closure temperature is relatively high (500 to 300˚C; Suzuki *et al.*, 1996) and the Re-Os system within

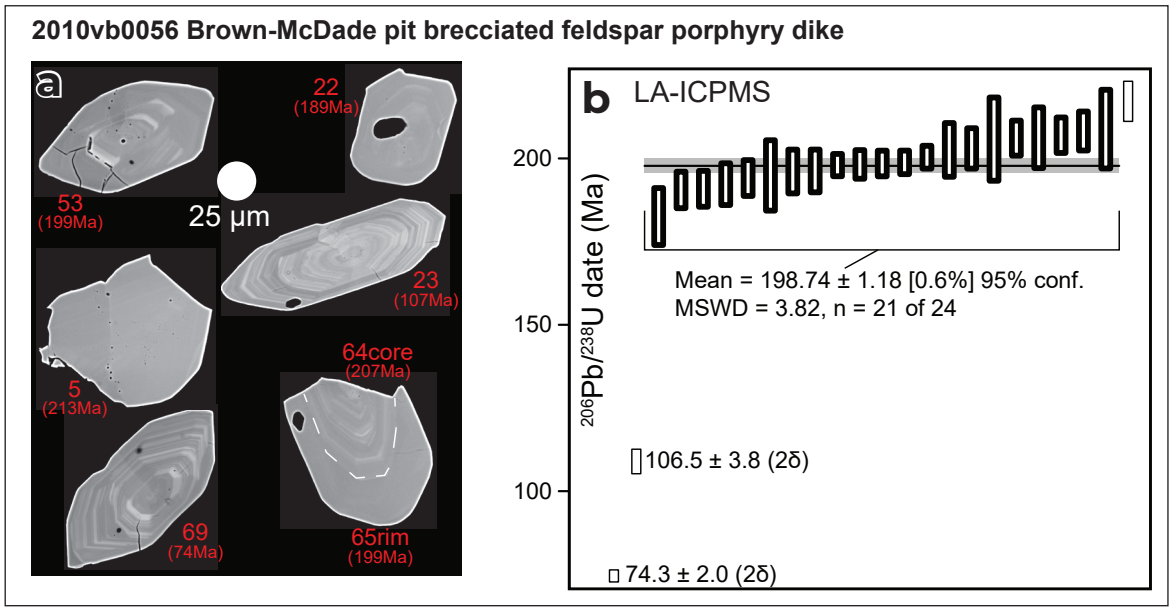

Figure 16. *U-Pb zircon geochronology results from 2010v0056, brecciated feldspar porphyry dike from the Brown-McDade pit.* ***(a)*** *BSE images of zircon analyzed by LA-ICPMS (red analysis number with $^{206}Pb/^{238}U$ date in smaller text below).* ***(b)*** *Ranked plot of $^{206}Pb/^{238}U$ dates determined by LA-ICPMS. The light grey band around Concordia (dark grey line) shows the decay constant uncertainties. Analyses included in weighted mean age (light grey horizontal bar) calculations are bold; analyses with thin lines are not used in calculations. Errors are at 2σ. MSWD = mean squared weighted deviation, n = number of analyses included in age calculation.*

Table 4. *Lead isotope data table.*

Sample	Pluton/ Location	Suite	Lithology	Age (Ma)	Age control	Latitude	Longitude	Mineral
20PS218-1	Dickson plug	Whitehorse	quartz ± feldspar porphyry	111	estimated	62.05655	-137.15871	feldspar-sericite
20PS218-1	Dickson plug	Whitehorse	quartz ± feldspar porphyry	111	estimated	62.05655	-137.15871	feldspar-sericite
20PS218-1	Dickson plug	Whitehorse	quartz ± feldspar porphyry	111	estimated	62.05655	-137.15871	feldspar-quartz
20PS195-1	Bow Creek granite	Whitehorse	quartz-feldspar porphyritic biotite granite	108	dated	62.17610	-137.28290	feldspar
19PS005-1	Klaza	Minto	hornblende ± biotite granodiorite	197	estimated	62.13802	-137.21842	feldspar
19PS024-1	Klaza	Minto	hornblende ± biotite granodiorite	198	estimated	62.13970	-137.20445	feldspar
19PS070-1	Mount Victoria	Mount Nansen	plagioclase-pyroxene porphyrytic andesite	115	estimated	62.11907	-137.17357	feldspar
KL15-291-208m	Klaza hill	Whitehorse	biotite-hornblende granodiorite	107	estimated	62.12315	-137.27227	feldspar
KL15-291-208m	Klaza hill	Whitehorse	biotite-hornblende granodiorite	108	estimated	62.12315	-137.27227	feldspar

Table 4 *continued.*

Sample	$^{206}Pb/^{204}Pb$	Error absolute	Error (%; 2δ)	$^{207}Pb/^{204}Pb$	Error absolute	Error (%; 2δ)	$^{208}Pb/^{204}Pb$	Error absolute	Error (%; 2δ)	$^{207}Pb/^{206}Pb$	Error absolute	Error (%; 2δ)	$^{208}Pb/^{206}Pb$	Error absolute	Error (%; 2δ)
20PS218-1	26.800	0.0110	0.04	16.050	0.0049	0.03	42.267	0.0178	0.04	0.5989	0.0002	0.027	1.5772	0.0002	0.010
20PS218-1	25.824	0.2421	0.94	15.921	0.0877	0.55	44.474	0.5053	1.14	0.6165	0.0047	0.759	1.7222	0.0111	0.642
20PS218-1	26.691	0.0926	0.35	15.969	0.0536	0.34	42.139	0.1876	0.45	0.5983	0.0006	0.093	1.5788	0.0044	0.279
20PS195-1	19.351	0.0053	0.03	15.728	0.0037	0.02	39.280	0.0122	0.03	0.8128	0.0001	0.014	2.0298	0.0003	0.015
19PS005-1	18.960	0.0034	0.02	15.681	0.0027	0.02	38.859	0.0082	0.02	0.8271	0.0000	0.006	2.0496	0.0002	0.011
19PS024-1	18.846	0.0014	0.01	15.600	0.0010	0.01	38.548	0.0030	0.01	0.8277	0.0000	0.004	2.0454	0.0001	0.003
19PS070-1	19.265	0.0027	0.01	15.659	0.0017	0.01	39.151	0.0061	0.02	0.8128	0.0001	0.008	2.0323	0.0001	0.007
KL15-291-208m	19.305	0.0118	0.06	15.692	0.0089	0.06	39.462	0.0248	0.06	0.8128	0.0002	0.023	2.0441	0.0003	0.016
KL15-291-208m	19.225	0.0044	0.02	15.634	0.0032	0.02	38.923	0.0111	0.03	0.8132	0.0001	0.010	2.0246	0.0003	0.017

molybdenite is relatively resistant to subsequent alteration (Stein *et al.*, 2001). We use hydrothermal minerals with lower closure temperatures (Ar-Ar in mica and feldspar and U-Pb in calcite) as chronometers of waning hydrothermal activity, typically these are several m.y. younger than Re-Os molybdenite ages from the same system (*e.g.*, Selby *et al.*, 2002). We refer to interpreted ages subsequently using magmatic, mineralization and hydrothermal designations. The Pb isotopic composition of igneous feldspar is generally thought to be similar to that of sulphides genetically related to their causative intrusion, assuming closed system behavior, which can be useful for interpreting metal sources and fluid interaction in porphyry systems (Tosdal *et al.*, 1999).

Magmatism

The U-Pb zircon data presented here help refine the magmatic ages of Late Triassic to Early Jurassic and mid-Cretaceous igneous rocks in the Mount Nansen area (Table 2; Fig. 17). The Mount Nansen area records four main magmatic episodes, from oldest youngest these are:

1. Paleozoic: Simpson Range metaplutonic suite (365 to 350 Ma) and Finlayson assemblage (351 to 344 Ma) and Sulphur Creek (264 to 252 Ma) metaplutonic suite;
2. Late Triassic to Early Jurassic: Pyroxene Mountain (220 to 214 Ma), Minto (205 to 194 Ma) and Long Lake (188 to 184 Ma) suites;
3. Mid-Cretaceous: Mount Nansen group (115 to 107 Ma) and Whitehorse suite (111 to 105 Ma); and
4. Late Cretaceous: Casino suite (78 to 74 Ma), Carmacks group (73 to 68 Ma) and Prospector Mountain suite (72 to 68 Ma).

The sample of deformed hornblende-biotite granodiorite collected from the Brown-McDade pit is 199.06 ± 0.96 Ma, within the range of the Minto suite regionally (205–194 Ma; Sack *et al.*, 2020). The second sample from the Brown-McDade pit is a quartz-feldspar porphyry, similar to both the mid and Late Cretaceous dikes seen near the Flex and Klaza deposits. The vast majority of the zircons in the sample are inherited, and based on the 198.74 ± 1.18 Ma weighted mean age using 21 of 24 grains, are sourced primarily from Minto suite country rock. A single grain at 106 Ma and another at 74 Ma can't be interpreted with confidence, but likely indicate the dike is Cretaceous; refining further to the mid or Late Cretaceous is not possible with our data.

Our new LA-ICPMS U-Pb zircon 111 ± 1.8 Ma age for the Dickson Hill plug and the similar quartz-feldspar porphyritic texture between the plug and mineralized dikes within core from the Flex deposit confirm a mid-Cretaceous age for these rocks as suggested by Mortensen *et al.* (2016). Our two CA-TIMS ages of 107.86 ± 0.03 Ma and 107.96 ± 0.03 Ma for the core and border phases, respectively, of the Bow Creek granite refine the mid-Cretaceous crystallization age of that body. At the Klaza deposit, the medium-grained biotite granodiorite of the Mount Nansen pluton and associated feldspar porphyry dikes, are all coeval with crystallization ages between 107.17 and 106.22 Ma (including errors; Table 2). Mid-Cretaceous magmatic rocks represent a volcanic complex with Mount Nansen andesite at the base, intruded by high-level plugs and dikes such as those seen on Dickson Hill and the border phase of the Bow Creek granite. Subsequently, the more voluminous Dawson Range granodiorite phase intruded the volcanic pile, again at high crustal levels as suggested by the associated porphyritic dikes at the Klaza deposit.

We don't report any new Late Cretaceous ages here for the Mount Nansen area, but recent work by Mortensen *et al.* (2016) and Lee (2021); Sack *et al.*, 2022 demonstrate that in the Klaza cluster there are both Casino (78–74 Ma) and Prospector Mountain (72–68 Ma) age magmatic rocks. The Kelly porphyry, best exposed near Slate Creek, has a crystallization age of a *ca.* 78 Ma, whereas the Cyprus porphyry immediately east of the Kelly porphyry and best exposed near the headwaters of the East Fork of Nansen Creek, has a U-Pb zircon crystallization age of *ca.* 71 Ma.

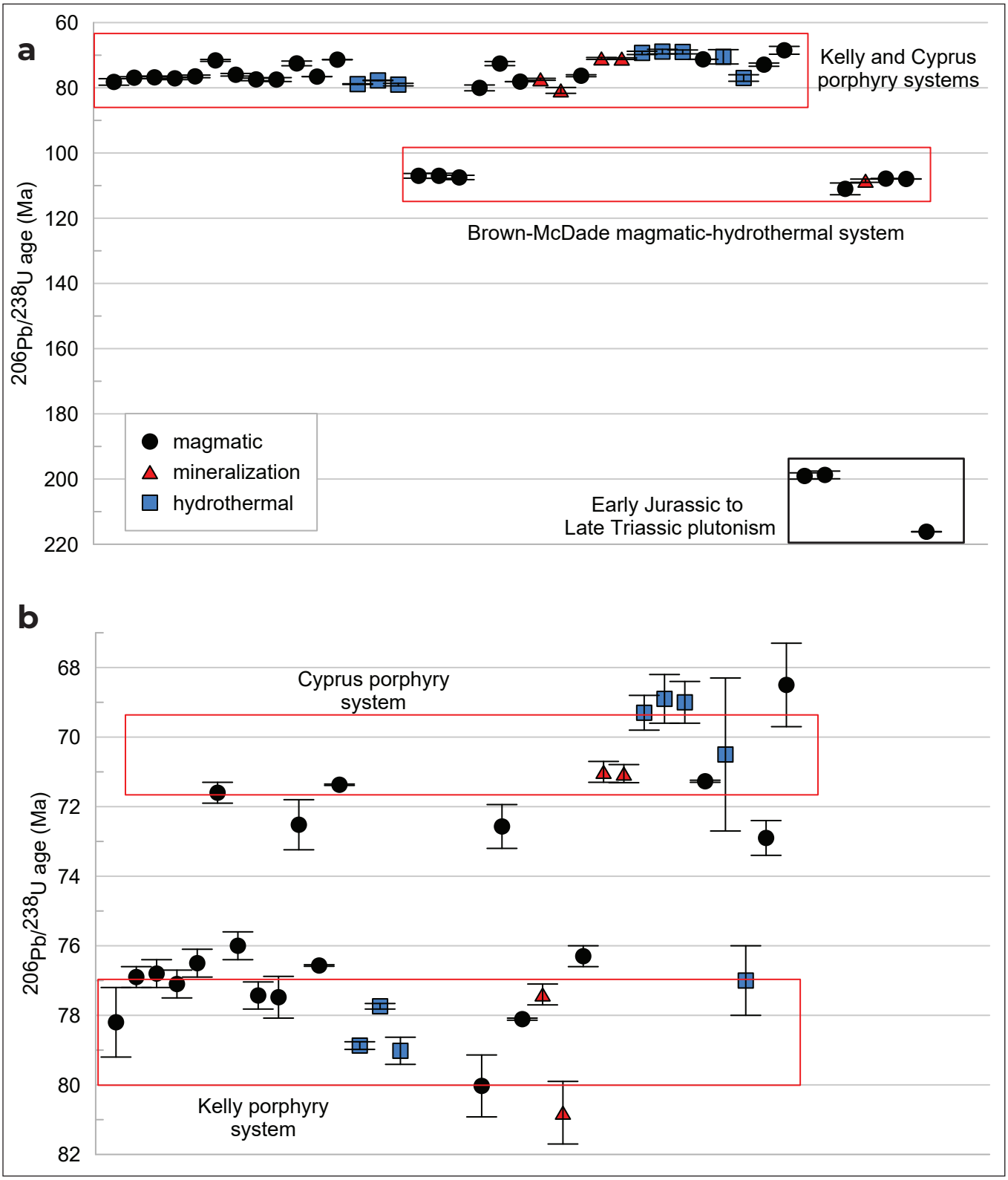

Figure 17. *Geochronology summary for the Mount Nansen area, not shown are Paleozoic ages for the ca. 365 to 350 Ma Simpson Range and ca. 264 to 252 Ma Sulphur Creek metaplutonic suites. Data plotted are from Mortensen et al. (2016), Joyce et al. (2015, 2020), Lee (2021) and this study. Ages symbolized by interpreted process; magmatic primarily U-Pb zircon analyses, mineralization Re-Os molybdenite analyses, hydrothermal U-Pb calcite and Ar-Ar muscovite. Error bars are 2δ. (a) Late Triassic to Late Cretaceous data. (b) Late Cretaceous data.*

Mineralization

A single MINFILE occurrence, Lucky Joe (115O 051), is associated with Paleozoic metaplutonic rocks of the Simpson Range 160 km northwest of the Mount Nansen area (Mortensen and Friend, 2020). Mineralization at Lucky Joe was ca. 352 to 333 Ma and mineralized rocks are clearly deformed (Mortensen and Friend, 2020). The Simpson Range metaplutonic suite is broadly coeval and cospatial with layered rocks of the Finlayson assemblage suggesting that these rocks were emplaced and deposited at an upper crustal level where porphyry system formation was possible. Furthermore, Simpson Range and Finlayson rocks are interpreted as having formed in an arc environment above a subduction zone (Piercey *et al.*, 2003) a setting permissive of porphyry system formation. Paleozoic mineral occurrences are not currently recognized in the Mount Nansen area. Rafts of rock mineralized in the Late Triassic are hosted by Minto suite intrusions 35 km to the northeast of the Mount Nansen area in the Carmacks Copper Belt (Kovacs *et al.*, 2020; Sack *et al.*, 2020). Though Minto suite intrusions are common in the Mount Nansen area, there are not any known Late Triassic mineral occurrences (Sack *et al.*, 2021).

Based on U-Pb zircon ages from mineralized dikes, previous workers have suggested the Mount Nansen area has both mid and Late Cretaceous deposits (Fig. 17; Mortensen *et al.*, 2016). The first direct mid-Cretaceous age for mineralization comes from vein-hosted molybdenite in the Flex deposit (ca. 108.5 Ma; Sack *et al.*, 2022). Brown-McDade, the other deposit in the Brown-McDade cluster, has not been directly dated and has low quality (K-Ar whole-rock) hydrothermal Late Cretaceous ages (Joyce *et al.*, 2015). In light of our equivocal U-Pb zircon data from a dike in the Brown-McDade pit, we can't refine a mid or Late Cretaceous age for mineralization at that deposit. However, based on the similar quartz-feldspar porphyry texture and the abundance of mid-Cretaceous dikes throughout the area (Mortensen *et al.*, 2016), we prefer the interpretation that mineralization in the Brown-McDade cluster was predominantly mid-Cretaceous, likely ca. 108.5 Ma.

Late Cretaceous mineralization appears to have been located primarily near the headwaters of Nansen Creek in the Klaza cluster (Fig. 2). Immediately east of Nansen Creek, chalcopyrite-molybdenite stock work veining associated with the Kelly porphyry has Re-Os ages between 81.7 and 75.9 Ma (Fig. 17; including errors; Lee, 2021). Immediately west of Nansen Creek, chalcopyrite-molybdenite stock work veining within the Cyprus porphyry has Re-Os molybdenite ages ranging from 71.3 to 70.7 Ma (Fig. 17; including errors; Selby and Creaser, 2001). Vein mineralization at the Klaza deposit is younger than the dikes in the area with U-Pb zircon, calcite and Ar-Ar muscovite ages between 77.8 and 70.1 Ma indicating a Late Cretaceous age, likely related to Prospector Mountain suite magmatism (Fig. 17).

Figure 18a,b shows the Pb isotopic ratios of the nine igneous feldspars analyses in the present study. Figure 18c, shows Pb isotopic ratios for igneous feldspar from other plutonic suites. Figure 18d and e show Pb isotopic ratios of galena from throughout the Dawson Range. The feldspar Pb isotopic analyses are divided by plutonic suite, primarily based on the U-Pb zircon magmatic ages, but because the age of all intrusions are not well constrained, suite assignment for some samples is interpreted. The shaded fields on each figure represent the majority of the data in each plutonic suite. The galena Pb isotopic analyses are symbolized first by mineralization age (shape) and deposit (colour). Again, because the age of mineralization is not well constrained for many deposits, age assignments are interpreted. For broader context, the shale curve of Godwin and Sinclair (1982) which closely approximates the Pb isotopic evolution of upper crustal rocks in the northern Cordillera (including the Yukon-Tanana terrane; Mortensen *et al.*, 2006) is shown in Figure 18a–e. The feldspar in sample 20PS218-1 are clay altered and these analyses are not considered to reflect magmatic conditions and are excluded from discussion.

Feldspar from rocks of Minto and Whitehorse suites in our study and other studies have $^{206}Pb/^{204}Pb$ ratios that range from 19.351 to 19.846 and define fields that broadly become more radiogenic with time. On $^{206}Pb/^{204}Pb$ versus $^{207}Pb/^{204}Pb$ diagrams (Fig. 18a,c,d),

most plutonic suites found in the Mount Nansen are plot below the shale curve of Godwin and Sinclair (1982), the exception is the mid-Cretaceous Whitehorse suite which plots above and below the curve. Similar grouping of feldspar isotopic compositions by plutonic suite is evident in the $^{206}Pb/^{204}Pb$ versus $^{208}Pb/^{204}Pb$ plot (Fig. 18b); $^{208}Pb/^{204}Pb$ ratios are positively correlated with increasing $^{206}Pb/^{204}Pb$, indicating an increasing radiogenic component with decreasing age. Mid-Cretaceous Whitehorse suite feldspars yielded the most radiogenic ratios. All three Cretaceous suites in the Mount Nansen area, Whitehorse, Casino and Prospector Mountain have similar feldspar Pb isotopic compositions, the Prospector Mountain suite may be slightly more radiogenic than the Whitehorse and Casino suites (Fig. 18c). The Pb isotopic compositions of galena from Cretaceous deposits (Fig. 18d,e) plot below the shale curve of Godwin and Sinclair (1982) and broadly overlap the field of feldspar Pb compositions from Cretaceous intrusions. As pointed out by Mortensen *et al.* (2016) these deposits are hosted by a variety of rocks and the age of mineralization is commonly poorly constrained, thus linking metal sources directly between plutonic suites and deposits in the Dawson Range is challenging. However, coeval feldspar and galena broadly have similar Pb isotopic ratios suggesting the magmatic rocks were a significant source of metals. We note that the existing Pb isotopic data for plutonic rocks in the Dawson Range includes more whole-rock data (*e.g.*, Selby *et al.*, 1999; Smuk, 1999) than feldspar data which has complicated previous interpretations (*e.g.*, Mortensen *et al.*, 2016). Additional Pb isotopic data from well constrained magmatic feldspar are required to refine interpretations further.

Conclusions

The U-Pb zircon and Pb isotopic data presented here refine understanding of magmatism and mineralization in the Mount Nansen area with the following conclusions:

1. The Brown-McDade deposit is hosted by Minto suite granodiorite with a crystallization age of 199.06 Ma and is intruded by dikes which likely have a Cretaceous emplacement age;
2. Magmatism and mineralization on Dickson Hill and at the adjacent Flex deposit (and likely other Brown-McDade cluster deposits) were mid-Cretaceous, *ca.* 108.5 Ma;
3. The Mount Nansen pluton is a composite Whitehorse suite body which includes a relatively small Bow Creek granite phase and a widespread Dawson Range granodiorite phase.
    a. Bow Creek granite phase is zoned with the border phase crystallizing at 107.86 Ma, slightly after the central phase which crystallized at 107.96 Ma; and
    b. Dawson Range granodiorite phase crystallized 107 to 105 Ma;
4. Mid-Cretaceous magmatism likely began with eruption of dominantly andesitic volcanic rocks, followed by intrusion of felsic, high-level porphyritic dikes and plugs such as those seen at Dickson Hill and possibly the margins of the Bow Creek body. The mid-Cretaceous magmatic cycle ended with emplacement of widespread intermediate plutonic rocks that are dominantly equigranular and fine to medium-grained. The increase in size of plutonic bodies and lack of porphyritic textures may suggest a slightly deeper emplacement level for the main Dawson Range granodiorite phase in the Mount Nansen area. The smaller, slightly older and porphyritic phases may represent a high emplacement level and thus be more prospective for porphyry and related vein deposits;
5. Feldspar Pb isotopic data throughout the Dawson range becomes more radiogenic with time and are distinct for Late Triassic to Early Jurassic plutonic rocks versus Cretaceous plutonic rocks; and
6. Cretaceous feldspar isotopic data broadly overlaps Pb isotopic values of galena from deposits throughout the Dawson Range suggesting coeval magmatic rocks are a significant source of metals.

Acknowledgements

The authors thank Matt van Loon for geology discussion and Rockhaven Resources for data sharing and hospitality.

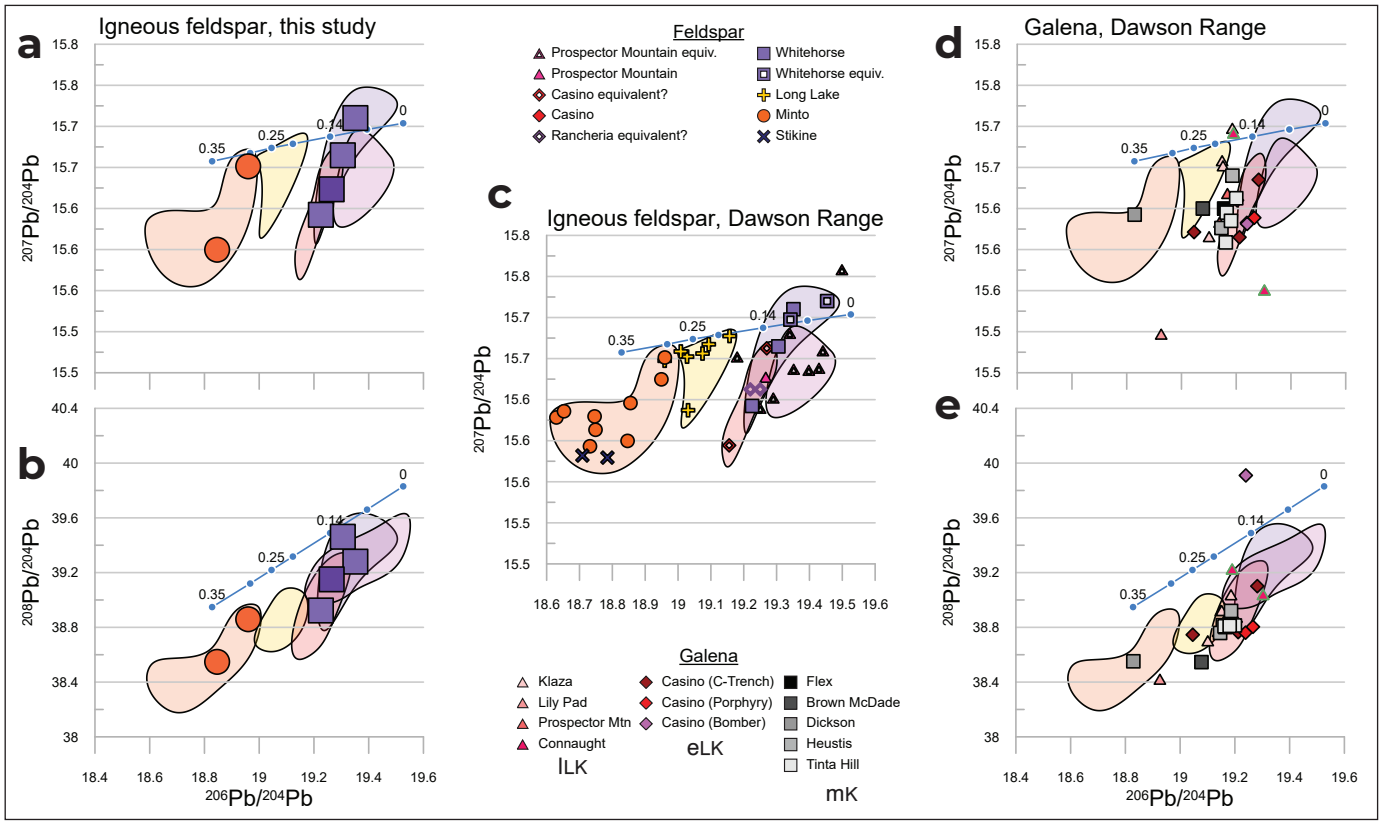

Figure 18. *$^{206}Pb/^{204}Pb$ versus $^{207}Pb/^{204}Pb$ and $^{206}Pb/^{204}Pb$ versus $^{208}Pb/^{204}Pb$ plots.* ***(a** and **b)** From this study; data for feldspar Pb are given in Table 4.* ***(c)** From plutonic rocks throughout the Dawson range and east-central Alaska; data from feldspar Pb are from Rasmussen (2013), Mortensen et al. (2016), Dusel-Bacon et al. (2015) and Sack et al. (2020).* ***(d** and **e)** From galena in vein deposits in the Mount Nansen area; data are from Smuk (1999) and Mortensen et al. (2016).*

References

Allan, M.A. and Friend, M., 2018. Bedrock geological map of the Mount Freegold district, Dawson Range (NTS 115I/6 and parts of 115I/2,3,5,7,10,11,12). Yukon Geological Survey, Open File 2018-2, scale 1:50 000.

Aurora Geosciences and Bruce, J.O., 2020. Residual total magnetic field, shaded colour contour map (NTS 115I). *In:* Reprocessing of Yukon magnetic data for NTS 115I. Yukon Geological Survey, Open File 2020-33, sheet 2 of 4.

Bennett, V. and Tubrett, M., 2010. U-Pb isotopic age dating by LAM ICP-MS, INCO Innovation Centre, Memorial University: Sample preparation methodology and analytical techniques *In*: Yukon Exploration and Geology 2009, K.E. MacFarlane, L.H. Weston and L.R. Blackburn (eds.), Yukon Geological Survey, p. 47–55.

Carlson, G.G., 1987. Geology of Mount Nansen (115-I/3) and Stoddart Creek (115-I/6) map areas Dawson Range, central Yukon. Exploration and Geological Services Division, Yukon Region, Indian and Northern Affairs Canada, Open File 1987-2, 194 p.

Clark, A.D., 2017. Tectonometamorphic history of mid-crustal rocks at Aishihik Lake, southwest Yukon. MSc thesis, Simon Fraser University, 153 p.

Colpron, M., Gordey, S., Lowey, G., White, D. and Piercey, S., 2007. Geology of the northern Whitehorse trough, Yukon (105E/12, 13 and parts of 11 and 14; 105L/4 and parts of 3 and 5; parts of 115H/9 and 16; 115I/1 and part of 8). Yukon Geological Survey, Open File 2007-6, scale 1:150 000.

Colpron, M., Sack, P.J., Crowley, J., Allan, M. and Beranek, L.P., in press. Late Triassic to Jurassic magmatic and tectonic evolution of the Intermontane terranes in Yukon, northern Canadian Cordillera: Transition from arc to syn-collisional magmatism and post-collisional lithospheric delamination. Tectonics.

Crowley, J.L., Schoene, B. and Bowring, S.A., 2007. U-Pb dating of zircon in the Bishop Tuff at the millennial scale. Geology, vol. 35, p. 1123–1126.

Dusel-Bacon, C., Aleinikoff, J.N., Day, W.C. and Mortensen, J.K., 2015. Mesozoic magmatism and timing of epigenetic Pb-Zn-Ag mineralization in the western Fortymile mining district, east-central Alaska: Zircon U-Pb geochronology, whole-rock geochemistry, and Pb isotopes. Geosphere, vol. 11, p. 786–822.

Gaidies, F., Morneau, Y.E., Petts, D.C., Jackson, S.E., Zagorevski, A. and Ryan, J.J., 2020. Major and trace element mapping of garnet: Unravelling the conditions, timing and rates of metamorphism of the Snowcap assemblage, west-central Yukon. Journal of Metamorphic Geology, vol. 39, p. 133–164.

Godwin, C.I. and Sinclair, A.J., 1982. Average lead isotope growth curves for shale-hosted zinc-lead deposits, Canadian Cordillera. Economic Geology, vol. 77, p. 675–690.

Grond, H.C., Churchill, S.J., Armstrong, R.L., Harakal, J.E. and Nixon, G.T., 1984. Late Cretaceous age of the Hutshi, Mount Nansen, and Carmacks groups, southwestern Yukon Territory and northwestern British Columbia. Canadian Journal of Earth Sciences, vol. 21, p. 554–558.

Hodges, K.V., 2014. Geochronology and Thermochronology in Orogenic Systems. *In*: Treatise on geochemistry: The crust, H.D. Holland and K.K. Turekian (eds.), Elsevier Pergamon, p. 263–292.

Jaffey, A.H., Flynn, K.F., Glendenin, L.E., Bentley, W.C. and Essling, A.M., 1971. Precision measurements of half-lives and specific activities of ^{235}U and ^{238}U. Physical Review C, vol. 4, p. 1889–1906.

Joyce, N.L., Iraheta Muniz, P., Rayner, N.M. and Ryan, J.J., 2020. Geochronology of the Mount Nansen-Nisling River area, Yukon. Geological Survey of Canada, Open File 8614, 28 p.

Joyce, N.L., Ryan, J.J., Colpron, M., Hart, C.J.R. and Murphy, D.C., 2015. A compilation of $^{40}Ar/^{39}Ar$ age determinations for igneous and metamorphic rocks, and mineral occurrences from central and southeast Yukon. Geological Survey of Canada, Open File 7924.

Klöcking, M., Mills, L., Mortensen, J. and Roots, C., 2016. Geology of mid-Cretaceous volcanic rocks at Mount Nansen, central Yukon, and their relationship to the Dawson Range batholith. Yukon Geological Survey, Open File 2016-25, 37 p.

Kovacs, N., Allan, M.M., Crowley, J.L., Colpron, M., Hart, C.J.R., Zagorevski, A. and Creaser, R.A., 2020. Carmacks Copper Cu-Au-Ag deposit: mineralization and post-ore migmatization of a Stikine arc porphyry copper system in Yukon, Canada. Economic Geology, vol. 115, p. 1413–1422.

Lee, W.-S., 2021. Metallogeny and characterization of Late Cretaceous superimposed porphyry Cu-Au-Mo and epithermal Au-Ag systems in the Dawson Range, Yukon, Canada: Case study on the Klaza deposit. PhD thesis, Laurentian University, Sudbury, Ontario, Canada.

Lee, W.-S., Kontak, D.J., Richards, J.P. and Sack, P., 2020. Updated geology and porphyry copper potential of the Klaza deposit, Mount Nansen district (Yukon MINFILE 115I 067). *In*: Yukon Exploration and Geology 2019, K.E. MacFarlane (ed.), Yukon Geological Survey, p. 75–97.

Mattinson, J.M., 2005. Zircon U-Pb chemical abrasion ("CA-TIMS") method: combined annealing and multi-step partial dissolution analysis for improved precision and accuracy of zircon ages. Chemical Geology, vol. 220, p. 47–66.

Mortensen, J.K., Dusel-Bacon, C., Hunt, J.A. and Gabites, J., 2006. Lead isotopic constraints on the metallogeny of middle and late Paleozoic syngenetic base-metal occurrences in the Yukon-Tanana and Slide Mountain/Seventymile terranes and adjacent portions of the North American miogeocline. *In*: Paleozoic Evolution and Metallogeny of Pericratonic Terranes at the Ancient Pacific Margin of North America, Canadian and Alaskan Cordillera, M. Colpron and J.L. Nelson (eds.), Geological Association of Canada, p. 261–279.

Mortensen, J. and Friend, M., 2020. An overview of porphyry style deposits in Yukon. *In*: Porphyry deposits of the northwestern Cordillera of North America: a 25-year update, E.R. Sharman, J.R. Lang and J.B. Chapman (eds.), Canadian Institute of Mining, Metallurgy and Petroleum, p. 176–193.

Mortensen, J.K. and Gabites, J.E., 2002. Lead isotopic constraints on the metallogeny of southern Wolf Lake, southeastern Teslin and northern Jennings River map areas, Yukon and British Columbia: Preliminary results. *In*: Yukon Exploration and Geology 2001, D.S. Emond, L.H. Weston and L.L. Lewis (eds.), Exploration and Geological Services Division, Yukon Region, Indian and Northern Affairs Canada, p. 179–188.

Mortensen, J.K., Hart, C.J.R., Tarswell, J. and Allan, M.M., 2016. U-Pb zircon age and Pb isotopic constraints on the age and origin of porphyry and epithermal vein mineralization in the eastern Dawson Range, Yukon. *In*: Yukon Exploration Geology 2015, K.E. MacFarlane and M.G. Nordling (eds.), Yukon Geological Survey, p. 165–185, including appendices.

Mottram, C.M., Kellett, D.A., Barresi, T., Zwingmann, H., Friend, M., Todd, A. and Percival, J.B., 2020. Syncing fault rock clocks: Direct comparison of U-Pb carbonate and K-Ar illite fault dating methods. Geology, vol. 48, p. 1179–1183.

Piercey, S.J. and Colpron, M., 2009. Composition and provenance of the Snowcap assemblage, basement to the Yukon-Tanana terrane, northern Cordillera: Implications for Cordilleran crustal growth. Geosphere, vol. 5, p. 439–464.

Piercey, S.J., Mortensen, J.K. and Creaser, R.A., 2003. Neodymium isotope geochemistry of felsic volcanic and intrusive rocks from the Yukon–Tanana Terrane in the Finlayson Lake Region, Yukon, Canada. Canadian Journal of Earth Sciences, vol. 40, p. 77–97.

Rasmussen, K.L., 2013. The timing, composition and petrogenesis of syn- to post-accretionary magmatism in the northern Cordilleran miogeocline, eastern Yukon and southwest Northwest Territories. PhD thesis, University of British Columbia, 810 p.

Ryan, J.J., Israel, S., Williams, S.P., Parsons, A.J. and Hayward, N., 2018. Bedrock geology, Klaza River area, Yukon. Geological Survey of Canada, Canadian Geoscience Map 376, scale 1:100 000.

Ryan, J.J., Westberg, E.E., Williams, S.P. and Chapman, J.B., 2016. Geology, Mount Nansen - Nisling River area, Yukon. Geological Survey of Canada, Canadian Geoscience Map 292 (ed. prelim.), 1 sheet, scale 1:100 000.

Ryan, J., Zagorevski, A., Williams, S.P., Root, C.F., Ciolkiewicz, W. and Chapman, J.B., 2013. Geology, Stevenson Ridge (northeast part), Yukon. Geological Survey of Canada, Geoscience map 116 (2nd edition, preliminary), scale 1:100 000.

Sack, P.J., Colpron, M., Crowley, J.L., Ryan, J.J., Allan, M.M., Beranek, L.P. and Joyce, N.L., 2020. Atlas of Late Triassic to Jurassic plutons in the Intermontane terranes of Yukon. Yukon Geological Survey, Open File 2020-1, 378 p.

Sack, P.J., Eriks, N. and van Loon, S., 2021. Revised geological map of the Mount Nansen area (NTS 115I/3 and part of 115I/2). Yukon Geological Survey, Open File 2021-2, 2 sheets; scales 1:50 000 and 1:20 000.

Sack, P.J., Eriks, N. and van Loon, S., 2022. Updated geological map of the Mount Nansen area (NTS 115I/3 and part of 115I/2). Yukon Geological Survey, Open File 2022-4, 2 sheets; scales 1:50 000 and 1:20 000.

Sawyer, J.P.B. and Dickinson, R.A., 1976. Mount Nansen. *In*: Porphyry deposits of the Canadian Cordillera, S.A. Brown (ed.), The Canadian Institute of Mining and Metallurgy, Special Volume 15, p. 336–343.

Schmitz, M.D. and Schoene, B., 2007. Derivation of isotope ratios, errors and error correlations for U-Pb geochronology using 205Pb-235U-(233U)-spiked isotope dilution thermal ionization mass spectrometric data. Geochemistry, Geophysics, Geosystems (G^3), vol. 8, Q08006, doi:10.1029/2006GC001492.

Selby, D. and Creaser, R.A., 2001. Late and mid-Cretaceous mineralization in the northern Canadian Cordillera: Constraints from Re-Os molybdenite dates. Economic Geology, vol. 96, p. 1461–1467.

Selby, D., Creaser, R.A., Hart, C.J.R., Rombach, C.S., Thompson, J.F.H., Smith, M.T., Bakke, A.A. and Goldfarb, R.J., 2002. Absolute timing of sulfide and gold mineralization: A comparison of Re-Os molybdenite and Ar-Ar mica methods from the Tintina Gold Belt, Alaska. Geology, vol. 30, p. 791–794.

Selby, D., Creaser, R.A. and Nesbitt, B.E., 1999. Major and trace element compositions and Sr–Nd–Pb systematics of crystalline rocks from the Dawson Range, Yukon, Canada. Canadian Journal of Earth Sciences, vol. 36, p. 1463–1481.

Smuk, K.A., 1999. Metallogeny of epithermal gold and base metal veins of the southern Dawson Range, Yukon. MSc thesis, McGill University, 188 p.

Staples, R.D., Murphy, D.C., Gibson, H.D., Colpron, M., Berman, R.G. and Ryan, J.J., 2014. Middle Jurassic to earliest Cretaceous mid-crustal tectono-metamorphism in the northern Canadian Cordillera: Recording foreland-directed migration of an orogenic front. Geological Society of America Bulletin, vol. 126, p. 1511–1530.

Stein, H.J., Markey, R.J., Morgan, J.W., Hannah, J.L. and Scherstén, A., 2001. The remarkable Re–Os chronometer in molybdenite: how and why it works. Terra Nova, vol. 13, p. 479–486.

Suzuki, K., Shimizu, H. and Masuda, A., 1996. ReOs dating of molybdenites from ore deposits in Japan: Implication for the closure temperature of the ReOs system for molybdenite and the cooling history of molybdenum ore deposits. Geochimica et Cosmochimica Acta, vol. 60, p. 3151–3159.

Tosdal, R.M., Wooden, J.L. and Bouse, R.M., 1999. Pb isotopes, ore deposits, and metallogenic terranes. *In*: Application of Radiogenic Isotopes to Ore Deposit Research and Exploration, Reviews in Economic Geology, Volume 12, D.D. Lambert and J. Ruiz (eds.), Society of Economic Geology, p. 1–28.

YGS, 2020. Yukon Digital Bedrock Geology. Yukon Geological Survey, https://data.geology.gov.yk.ca/Compilation/3#InfoTab, [accessed March 31, 2020].

Appendices

The appendices are only available as digital files. They are included in a .zip file that accompanies this document, and are available from https://data.geology.gov.yk.ca.

Appendix 1 – magnetic susceptibility

Appendix 2 – U-Pb zircon geochronology